transduction. This result showed that the ES-EB- or iPS-EB-derived cells could express transgenes by Ad vectors, and that Ad vector mediated the transient transgene expression in these cells.

Transient HoxB4 expression augments the generation of hematopoietic cells from mouse ES and iPS cells

To induce and expand the hematopoietic cells from the iPS cell line 38C2, EB-derived total cells were plated and cultured on OP9 stromal cells with the hematopoietic cytokines. On day 10 after plating on OP9 cells, the number of 38C2-derived hematopoietic cells in LacZ-transduced cells was similar to that in non-transduced cells. On the other hand, transient transduction of HoxB4 with Ad-hHoxB4 resulted in a significant increase in the number of hematopoietic cells compared with non-transduced cells or LacZ-transduced cells (Fig. 2a, middle). Likewise, an increase in the hematopoietic cell number by Ad vector-mediated hHoxB4 transduction was also observed in ES cell derived-hematopoietic cells or the other iPS line 20D17-derived hematopoietic cells (Fig. 2a, left and right). Additionally, ES-EB- or iPS-EB-derived $CD41^+c\text{-}kit^+$ cells, which were transiently transduced with hHoxB4, could proliferate on OP9 stromal cells for over 20 days (Fig. 2b). This result is mostly in agreement with the previous report that ES cell-derived hematopoietic cells stably expressing HoxB4 had a growth advantage in the presence of hematopoietic cytokines (Pilat et al., 2005). Transient, but not stable, HoxB4 expression in ES-EB- or iPS-EB-derived cells would be sufficient to augment the generation of hematopoietic cells from ES and iPS cells.

We next investigated the surface antigen expression in non-transduced cells, LacZ-transduced cells, or hHoxB4-transduced cells after expansion on OP9 stromal cells. Flow cytometric analysis revealed an increase of CD45 and CD41 expressions in HoxB4-transduced cells, compared with non-transduced cells and LacZ-transduced cells (Figs. 3a and b). CD45 is known as a marker of hematopoietic cells. In both *in vitro* ES cell differentiation and a developing mouse embryo, the expression of CD45 was developmentally controlled, and CD45 expression was observed on hematopoietic cells after expression of CD41 (Mitjavila-Garcia et al., 2002; Mikkola et al., 2003). Thus, a higher percentage of $CD45^+$ cells in HoxB4-transduced cells would be due, at least in part, to an increase of CD41 expression in HoxB4-transduced cells relative to non-transduced cells and LacZ-transduced cells. We also found a significant elevation of Sca-1 in hHoxB4-transduced cells (Figs. 3a and b). Sca-1 is expressed in fetal and adult HSPCs (Arai et al., 2004; McKinney-Freeman et al., 2009), although Sca-1 expression was observed in other types of cells. Therefore, our data suggest that immature hematopoietic cells would be generated in hHoxB4-transduced cells more efficiently than in non-transduced cells or LacZ-transduced cells.

In parallel with the flow cytometric analysis, we also analyzed the expression levels of hematopoietic marker genes in iPS cell-derived hematopoietic cells by RT-PCR (Fig. 3c). The expression levels of marker genes in LacZ-transduced cells were mostly equal to those in non-transduced cells. In contrast, among the genes we assayed, the expression levels of *Gata-1*, *c-myb*, and *Cxcr4* mRNA were slightly but significantly up-regulated in hHoxB4-transduced cells. GATA-1 reflects early hematopoietic development, whereas c-Myb is a marker of definitive hematopoiesis (Godin and Cumano, 2002). Increased expression of these genes in HoxB4-transduced cells suggests that transient hHoxB4 expression promotes the production of both primitive and definitive hematopoietic progenitor cells from mouse ES and iPS cells. We could not detect the hHoxB4 mRNA expression in Ad-hHoxB4-transduced cells, confirming the transient hHoxB4 expression by Ad vectors (Fig. 3c).

HoxB4 expression enhances development of hematopoietic progenitor cells from mouse ES and iPS cells

To examine whether hematopoietic immature cells with hematopoietic colony-forming potential could be generated from ES and iPS cells, ES cell-derived hematopoietic cells and iPS cell-derived hematopoietic cells, both of which were cultured on OP9 stromal cells for 10 days, were plated and cultured in methylcellulose-containing media with hematopoietic cytokines. Without Ad transduction, the number of total hematopoietic colonies in the iPS cell line 38C2 was five times as high as that in ES cells, whereas another iPS cell line, 20D17, had nearly the same hematopoietic differentiation potential as ES cells (Fig. 4a). These results indicate that there is a difference in hematopoietic differentiation potential among iPS cell lines.

We next examined the hematopoietic colony potential in LacZ-transduced cells or HoxB4-transduced cells. The colony assay revealed a significant increase in the number of total hematopoietic colonies in hHoxB4-transduced cells compared with control cells, whereas there was no significant difference in the number of hematopoietic colonies between

Figure 1 Transduction with Ad vectors in ES-EB- or iPS-EB-derived cells. (a, b) The expression levels of CAR, a primary receptor for Ad, in ES-EB- or iPS-EB-derived total cells (a) or $CD41^+c\text{-}kit^+$ cells (b) were detected with anti-mouse CAR monoclonal antibody by flow cytometric analysis. As a negative control, the cells were incubated with an irrelevant antibody. Data shown are from one representative experiment of three performed. (c, d) EB-derived total cells (c) or $CD41^+c\text{-}kit^+$ cells (d), purified by FACS (Supplemental Fig. 1), were transduced with Ad-DsRed or Ad-GFP for 1.5 h, and transgene-expressing cells were then analyzed by flow cytometry. Because $CD41^+c\text{-}kit^+$ cells do not express GFP (Fig. 1b), Ad-GFP was used for transduction into $CD41^+c\text{-}kit^+$ cells. Similar results were obtained in three independent experiments. (e) The expression level of human HoxB4 mRNA in the cells was examined by conventional RT-PCR on days 3 and 6 after transduction with Ad-hHoxB4 at 3000 VPs/cell into EB-derived total cells. Abbreviations: ES, embryonic stem; iPS, induced pluripotent stem; mCAR, mouse coxsackievirus and adenovirus receptor; GFP, green fluorescent protein; Cont., control.; VP, vector particle; RT, reverse transcription; GAPDH, glyceraldehyde-3-phosphate dehydrogenase.Transduction with Ad vectors

non-transduced cells and LacZ-transduced cells (Fig. 4a). Note that the number of the most immature multipotent progenitor cells, CFU-GEMM/CFU-Mix, in hHoxB4-transduced cells was approximately seven times as great as that in non-transduced cells or LacZ-transduced cells, and that large CFU-Mix colonies were more frequently observed in hHoxB4-transduced cells than control cells (Fig. 4b and data not shown). A colony assay after culturing on OP9 stromal cells for 20 days also revealed that much number of myeloid (CFU-G, M, and GM) colonies and CFU-Mix colonies were observed by transient hHoxB4 transduction (Figs. 4c and d). Thus, our data clearly showed that Ad vector-mediated transient hHoxB4 expression

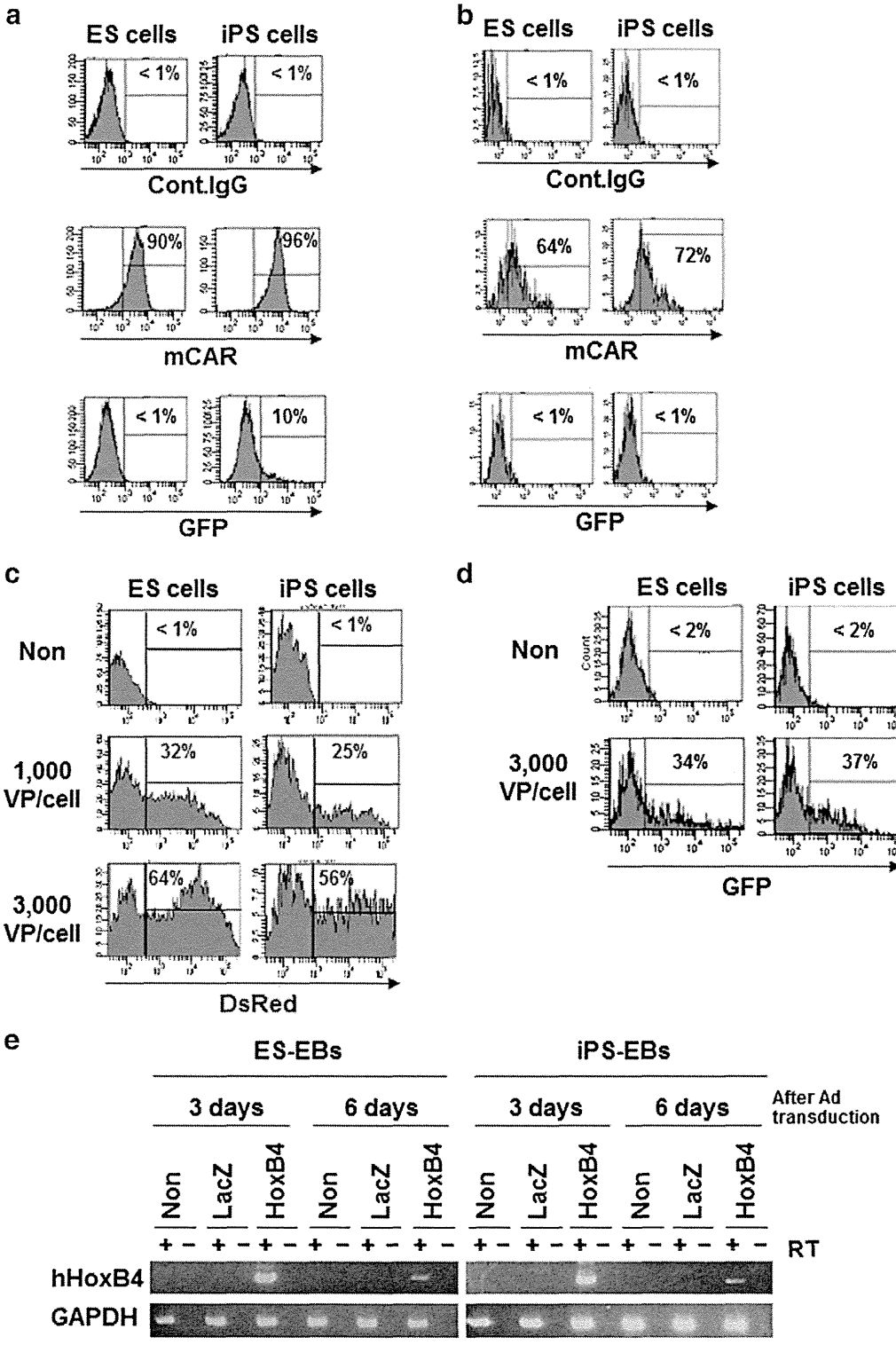

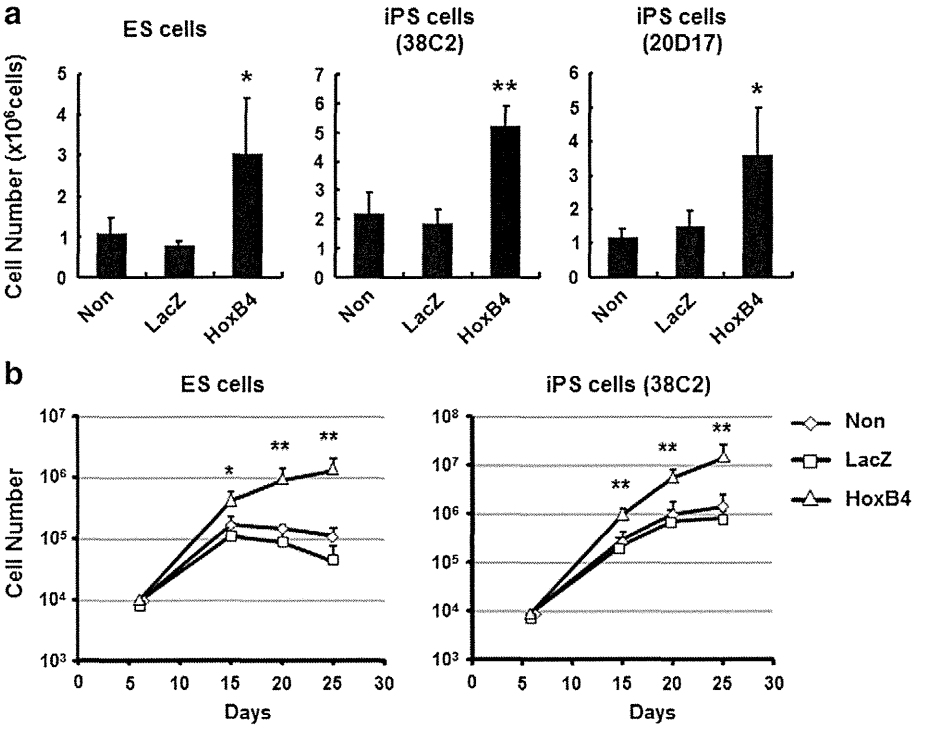

Figure 2 The number of ES cell- or iPS cell-derived hematopoietic cells was significantly increased in Ad-hHoxB4-transduced cells. (a, b) ES-EB- or iPS-EB-derived total cells (a) or CD41$^+$c-kit$^+$ cells (b) were transduced with Ad-LacZ or Ad-hHoxB4 at 3000 VPs/cell for 1.5 h, and the cells were then plated on OP9 feeder cells. As a control, non-transduced cells were also plated on OP9 cells. After culturing on OP9 feeders with the hematopoietic cytokines for 10 days (a) or 20 days (b), the number of hematopoietic cells per 2 wells of a 6-well plate was counted. (a) Left, ES cells; middle, iPS cell line 38C2; right, iPS cell line 20D17. Results shown were the mean of four independent experiments with indicated standard deviations. * $p<0.05$, ** $p<0.01$ as compared with non-transduced or Ad-LacZ-transduced cells.

enhances the differentiation of hematopoietic immature cells, including HSPCs, from mouse ES and iPS cells.

Discussion

Previous studies have shown that enforced expression of HoxB4 is an effective strategy for hematopoietic differentiation from both mouse and human ES cells (Kyba et al., 2002; Bowles et al., 2006; Pilat et al., 2005; Schiedlmeier et al., 2007). These studies usually used recombinant ES cells, such as ES cells constitutively expressing HoxB4 (Pilat et al., 2005) or ES cells containing a tetracycline (Tet)-inducible HoxB4 expression system (Kyba et al., 2002), to induce hematopoietic cells. However, this expression system might raise clinical concerns, including the risk of oncogenesis due to integration of transgenes into host genomes. In the present study, we showed that Ad vector-mediated transient hHoxB4 expression in mouse ES-EB- or iPS-EB-derived cells could result in an efficient production of hematopoietic cells, including HSPCs with a hematopoietic colony-forming ability, from mouse ES and iPS cells (Figs. 2, 3, and 4). Our data obtained in this report are largely consistent with previous reports (Kyba et al., 2002) in which HSPCs were generated by using ES cells containing the Tet-regulated HoxB4 expression cassette. Therefore, a transient HoxB4 expression system using an Ad vector, instead of a Tet-inducible HoxB4 expression system, would contribute to safer clinical applications of ES or iPS cell-derived hematopoietic cells.

Conventional Ad vector is known to infect the cells through an entry receptor, CAR, on the cellular surface (Bergelson et al., 1997; Tomko et al., 1997). Previously, we showed that undifferentiated ES and iPS cells expressed CAR, and conventional Ad vector could easily transduce a foreign gene in more than 90% of the undifferentiated ES and iPS cells at 3000 VPs/cell (Kawabata et al., 2005; Tashiro et al., 2009). Like undifferentiated ES and iPS cells, we could detect the CAR expression in more than 90% or 70% of EB-derived total cells or EB-derived CD41$^+$c-kit$^+$ cells, respectively (Figs. 1a and b). However, the transduction efficiency in EB-derived total cells or CD41$^+$c-kit$^+$ cells was only 60% or 40%, respectively, of the cells at most (Figs. 1c and d). Although we are not certain why transgene expression was not observed in all of CAR$^+$ EB-derived cells, it is possible that the promoter might not have worked in all of the cells because the EB-derived total cells and CD41$^+$c-kit$^+$ cells were heterogeneous, unlike in the case of undifferentiated ES and iPS cells. It is also possible that the Ad binding site of CAR might be disrupted by trypsin treatment during the preparation of the EB-derived cells (Carson, 2000). Because the development of efficient transduction methods in EB-derived cells is considered to be a powerful tool to promote the hematopoietic differentiation from ES and iPS cells, further improvement of the transduction conditions will be needed.

We found a difference in the hematopoietic differentiation potential among mouse iPS cell lines (Fig. 4). Consistent with our data, Kulkeaw et al. showed a difference in the hematopoietic differentiation capacity among six iPS cell lines (Kulkeaw et al., 2010). In addition, recent studies have reported that iPS cells leave an epigenetic memory of

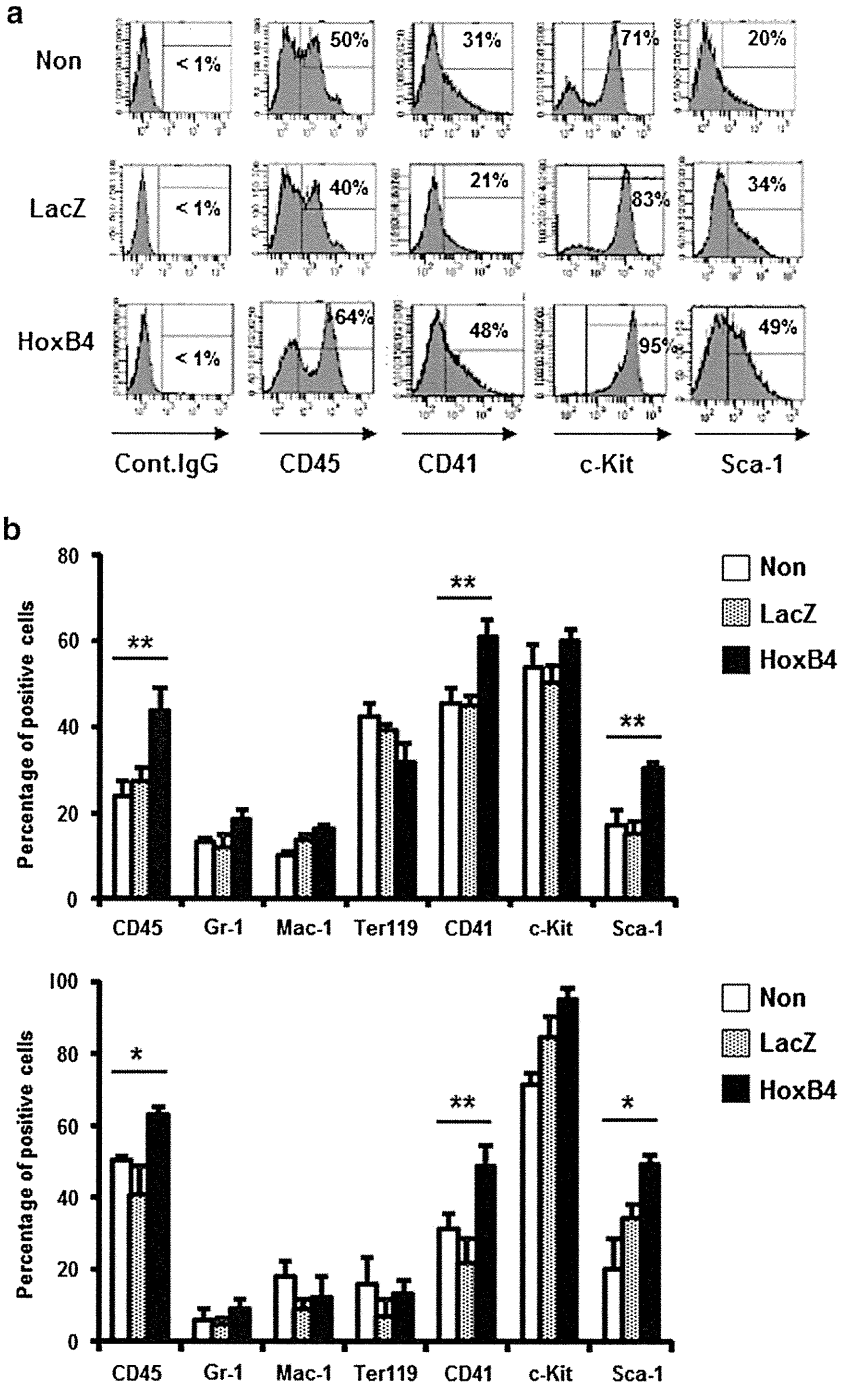

Figure 3 Expression of surface antigen and hematopoietic marker genes in mouse ES cell- or iPS cell-derived cells. (a, b) ES cell- or iPS cell line 38C2-derived cells were reacted with each antibody, and were then subjected to flow cytometric analysis. (a) Representative data from iPS cell line 38C2 are shown. (b) Percentage of each antigen positive cells in ES cell-derived cells (upper) or iPS cell-derived cells (lower) is shown. The data expressed the mean of three independent experiments with indicated standard deviations. * $p<0.05$, ** $p<0.01$ as compared with non-transduced or Ad-LacZ-transduced cells. (c) Total RNA was extracted from undifferentiated iPS cells (Day 0), iPS-EB (Day 5), iPS cells-derived hematopoietic cells (day 15), OP9 stromal cells, and MEF feeder, and semi-quantitative PCR (left) or quantitative real-time PCR (right) was then carried out as described in the Materials and methods. The data expressed the mean of three independent experiments with indicated standard deviations. * $p<0.05$, ** $p<0.01$ as compared with non-transduced or Ad-LacZ-transduced cells. Abbreviation: EBs, embryoid bodies; MEF, mouse embryonic fibroblast; GATA, GATA-binding protein.

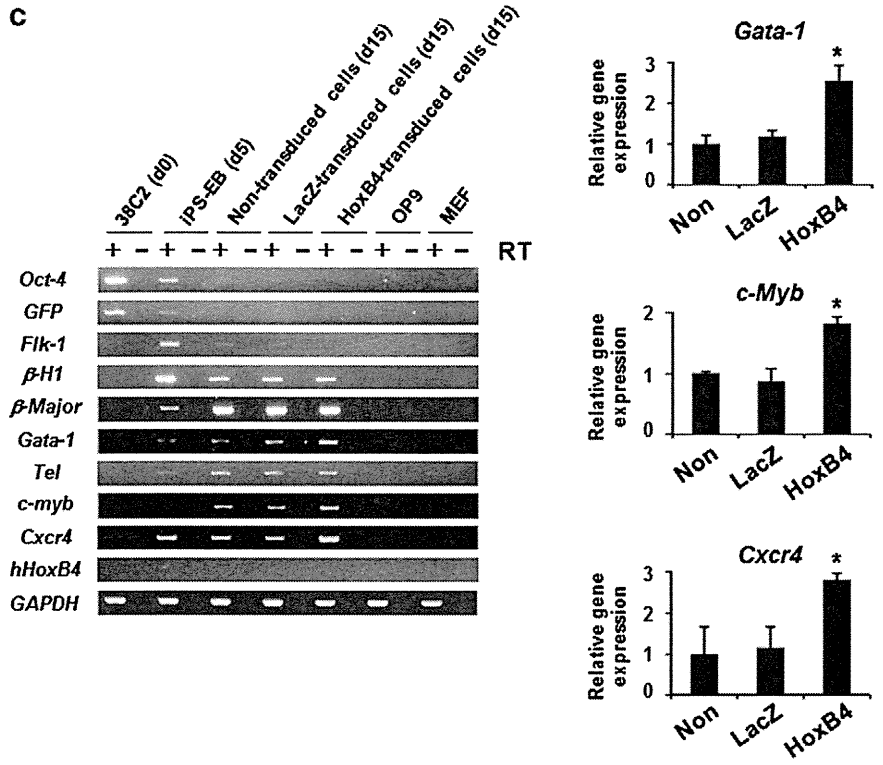

Figure 3 (*continued*).

their cellular origin, and this memory influences their functional properties, including *in vitro* differentiation (Kim et al., 2010; Polo et al., 2010). Thus, these reports indicate that, in order to obtain a large number of HSPCs from iPS cells, it is necessary to choose an appropriate iPS cell line, such as HSPC-derived iPS cells (Okabe et al., 2009). Importantly, using mouse embryonic fibroblast-derived iPS cells (38C2 and 20D17), we showed that the use of transient hHoxB4 transduction in iPS-EB-derived cells achieved more effective differentiation into HSPCs than the use of non-transduced cells (Fig. 4). Our method therefore should be efficient for the production of HSPCs from any iPS cell line.

An important but unsolved question in this study is whether ES cell-derived hematopoietic cells and iPS cell-derived hematopoietic cells transduced with Ad-hHoxB4 have long-term hematopoietic reconstitution potential *in vivo*. Recent studies have demonstrated that some surface antigen expressions were different between bone marrow-derived HSPCs and ES cell-derived HSPCs, and that $CD41^+$ cells had long-term repopulation ability in ES cell-derived HSPCs (McKinney-Freeman et al., 2009; Matsumoto et al., 2009). Our flow cytometric analysis revealed an increase of $CD41^+$ cells in hHoxB4-transduced cells compared with non-transduced cells and LacZ-transduced cells (Fig. 3b). We also showed that Ad-hHoxB4-transduced cells could proliferate on OP9 stromal cells more efficiently than control cells (Fig. 2). Thus, these results suggest that immature hematopoietic cells were generated by transient hHoxB4 transduction, and that hHoxB4-transduced cells might have reconstitution potential *in vivo*. This *in vivo* transplantation analysis is now on-going in our laboratory.

In the present study, we succeeded in the promotion of hematopoietic differentiation from mouse ES and iPS cells by Ad vector-mediated hHoxB4 transduction. Ad vector transduction can avoid the integration of transgene into host genomes, and multiple genes can be transduced by Ad vectors in an appropriate differentiation period. Thus, an even more efficient protocol for hematopoietic differentiation from ES and iPS cells could likely be established by co-transduction of HoxB4 and other genes involved in the hematopoiesis, such as Cdx4 (Wang et al., 2005) and Scl/Tal1 (Kurita et al., 2006), using Ad vectors. Taken together, our results show that Ad vector-mediated transient gene expression is valuable tool to induce hematopoietic cell from ES and iPS cells, and this strategy would be applicable to safe therapeutic applications, such as HSPC transplantation.

Materials and methods

Antibodies

The following primary monoclonal antibodies (Abs), conjugated with fluorescein isothiocyanate (FITC), phycoerythrin (PE), allophycocyanin (APC), or PE-Cy7, were used for flow cytometric analysis: anti-CD45 (30-F11, eBioscience, San Diego, CA), anti-CD11b (M1/70, eBioscience), anti-Sca-1 (D7, eBioscience), anti-Ter-119 (Ter-119, eBioscience), anti-Gr-1 (RB6-8C5, eBioscience), anti-c-Kit (ACK2 or 2B8, eBioscience), anti-CD41 (MWReg30, BD Bioscience San Jose, CA). Purified rat anti-coxsackievirus and adenovirus receptor (CAR) was kindly provided from Dr. T. Imai (KAN Research Institute, Hyogo, Japan). For detection of CAR, the PE-conjugated donkey anti-rat IgG (Jackson ImmunoResearch Laboratories, West

Grove, PA) or DyLight649-conjugated goat anti-rat IgG (BioLegend, San Diego, CA) was used as secondary Abs.

Cell cultures

The mouse ES cell line E14 and two mouse iPS cell lines, 38C2 and 20D17, both of which were generated by Yamanaka and his colleagues (Okita et al., 2007), were used in this study. 38C2 was kindly provided by Dr. S. Yamanaka (Kyoto University, Kyoto, Japan), and 20D17 was purchased from Riken Bioresource Center (Tsukuba, Japan). In the present study, we mainly used 38C2 iPS cells except where otherwise indicated. Mouse ES and iPS cells were cultured in leukemia inhibitory factor-containing medium on a feeder layer of mitomycin C-inactivated mouse embryonic fibroblasts (MEF) as described previously (Tashiro et al., 2009). OP9 stromal cells were cultured in α-minimum essential medium (αMEM: Sigma, St. Louis, MO) supplemented with 20% fetal bovine serum (FBS), 2 mM L-glutamine (Invitrogen, Carlsbad, CA), and non-essential amino acid (Invitrogen).

Ad vectors

Ad vectors were constructed by an improved *in vitro* ligation method (Mizuguchi and Kay, 1998, 1999). The shuttle

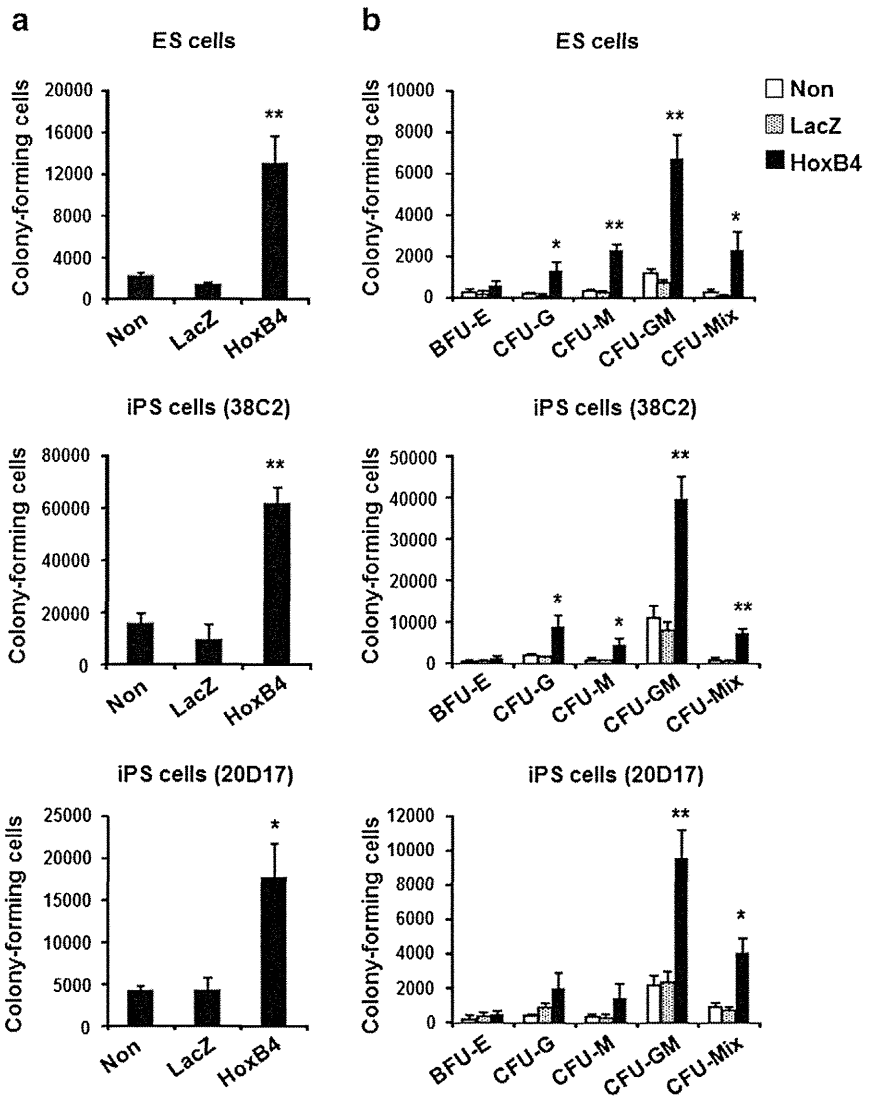

Figure 4 Significant increase of hematopoietic colony-forming cells in Ad-HoxB4-transduced hematopoietic cells. After ES-EB- or iPS-EB-derived cells were transduced with Ad-LacZ or Ad-hHoxB4, hematopoietic cells were generated by co-culturing with OP9 cells in the presence of hematopoietic cytokines for 10 days (a, b) or 20 days (c, d). A colony-forming assay was performed using methylcellulose medium, and the number of hematopoietic colonies was then counted under light microscopy. The number of total colonies (a, c) or subdivided colonies by morphological subtype (BFU-E, CFU-G, CFU-M, CFU-GM, and CFU-Mix) (b, d) generated from ES cells (E14) or iPS cells (38C2 and 20D17) was shown. Colony number was normalized to total number of the cells. Results shown were the mean of three (c, d) or four (a, b) independent experiments with indicated standard deviations. * $p<0.05$, ** $p<0.01$ as compared with non-transduced or Ad-LacZ-transduced cells. Abbreviation: BFU-E, burst-forming unit; CFU-G, colony-forming unit-granulocyte; CFU-M, CFU-monocyte; CFU-GM, CFU-granulocyte, monocyte; CFU-GEMM/CFU-Mix, CFU-granulocyte, erythrocyte, monocyte, megakryocyte.

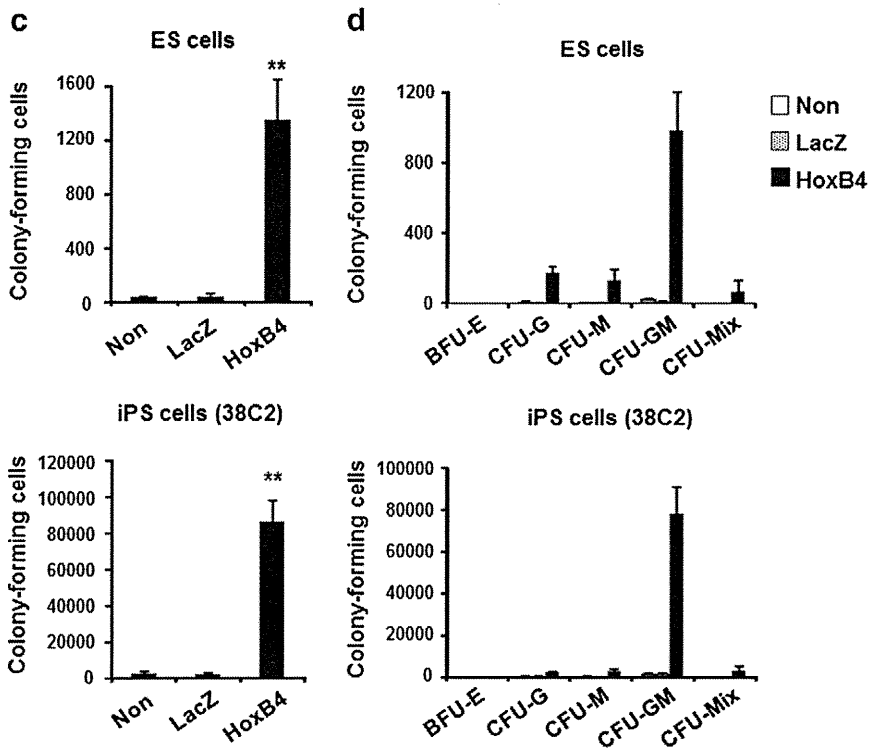

Figure 4 (*continued*).

plasmid pHMCA5, which contains the CMV enhancer/β-actin promoter with β-actin intron (CA) promoter (a kind gift from Dr. J. Miyazaki, Osaka University, Osaka, Japan) (Niwa et al., 1991), was previously constructed (Kawabata et al., 2005). The human HoxB4 (hHoxB4)-expressing plasmid, pHMCA-hHoxB4, and DsRed-expressing plasmid, pHMCA-DsRed, were generated by inserting a hHoxB4 cDNA (a kindly gift from Dr. S. Karlsson, Lund University Hospital, Lund, Sweden) and a DsRed cDNA (Clontech, Mountain View, CA), respectively, into pHMCA5. pHMCA-hHoxB4 or pHMCA-DsRed were digested with I-*Ceu*I/PI-*Sce*I and ligated into I-*Ceu*I/PI-*Sce*I-digested pAdHM4 (Mizuguchi and Kay, 1998), resulting in pAd-hHoxB4 or pAd-DsRed, respectively. Ad-hHoxB4 and Ad-DsRed were generated and purified as described previously (Tashiro et al., 2008). The CA promoter-driven β-galactosidase (LacZ)-expressing Ad vector, Ad-LacZ, and the CA promoter-driven GFP-expressing Ad vector, Ad-CA-GFP, were generated previously (Tashiro et al., 2008). The vector particle (VP) titer was determined by using a spectrophotometrical method (Maizel et al., 1968).

In vitro differentiation

Prior to embryoid body (EB) formation, mouse ES or iPS cells were suspended in differentiation medium (Dulbecco's modified Eagle's medium (Wako, Osaka, Japan) containing 15% FBS, 0.1 mM 2-mercaptoethanol (Nacalai tesque, Kyoto, Japan), 1×non-essential amino acid (Specialty Media, Inc.), 1×nucleosides (Specialty Media, Inc.), 2 mM L-glutamine (Invitrogen), and penicillin/streptomycin (Invitrogen)) and cultured on a culture dish at 37 °C for 45 min to remove MEF layers. Mouse ES cell- or iPS cell-derived EBs (ES-EBs or iPS-EBs, respectively) were generated by culturing ES or iPS cells on a round-bottom low cell binding 96-well plate (Lipidure-coat plate; Nunc) at 1×10^3 cells per well. ES-EBs or iPS-EBs were collected on day 5, and a single cell suspension was prepared by trypsin/EDTA treatment (Invitrogen) at 37 °C for 2 min. ES-EB- or iPS-EB-derived CD41$^+$c-kit$^+$ cells were sorted by FACSAria (BD Bioscience). The purity of the CD41$^+$c-kit$^+$ cells was greater than 90% based on flow cytometric analysis (Supplemental Fig. 1). Cells were then transduced with an Ad vector at 3000 vector particles (VPs)/cell for 1.5 h in a 15 ml tube. After transduction, total cells (2×10^5) or CD41$^+$c-kit$^+$ cells (1×10^4) were cultured on OP9 feeder cells in a well of a 6-well plate in αMEM supplemented with 20% FBS, 2 mM L-glutamine, non-essential amino acid, 0.05 mM 2-mercaptoethanol, and hematopoietic cytokines (50 ng/ml mouse stem cell factor (SCF), 50 ng/ml human Flt-3 ligand (Flt-3L), 20 ng/ml thrombopoietin (TPO), 5 ng/ml mouse interleukin (IL)-3, and 5 ng/ml human IL-6 (all from Peprotec, Rocky Hill, NJ)). After culturing with OP9 stromal cells, both non-adherent hematopoietic cells and adherent hematopoietic cells were collected as follows. The non-adherent hematopoietic cells were collected by pipetting and were transferred to 15 ml tubes. The adherent hematopoietic cells were harvested with the use of trypsin/EDTA, and then incubated in a tissue culture dish for 30 min to eliminate the OP9 cells. Floating cells were collected as hematopoietic cells and transferred to the same 15 ml tubes. These hematopoietic cells were kept on ice for further analysis.

Flow cytometry

Cells (1×10^5 to 5×10^5) were incubated with monoclonal Abs at 4 °C for 30 min and washed twice with staining buffer

Table 1 List of primers used for RT-PCR.

Gene name	Species	(5′) Sense primers (3′)	(5′)Antisense primers (3′)
GAPDH	Ms	ACCACAGTCCATGCCATCAC	TCCACCACCCTGTTGCTGTA
HoxB4	Hs	AGAGGCGAGAGAGCAGCTT	TTCCTTCTCCAGCTCCAAGA
Oct-3/4	Ms	GTTTGCCAAGCTGCTGAAGC	TCTAGCCCAAGCTGATTGGC
GFP	–	CACATGAAGCAGCACGACTT	TGCTCAGGTAGTGGTTGTCG
Flk-1	Ms	TCTGTGGTTCTGCGTGGAGA	GTATCATTTCCAACCACCC
Gata1	Ms	TTGTGAGGCCAGAGAGTGTG	TTCCTCGTCTGGATTCCATC
Gata1 (real-time PCR)	Ms	GTCAGAACCGGCCTCTCATC	GTGGTCGTTTGACAGTTAGTGCAT
Tel	Ms	CTGAAGCAGAGGAAATCTCGAATG	GGCAGGCAGTGATTATTCTCGA
c-myb	Ms	CCTCACCTCCATCTCAGCTC	GCTGGTGAGGCACTTTCTTC
β-H1	Ms	AGTCCCCATGGAGTCAAAGA	CTCAAGGAGACCTTTGCTCA
β-Major	Ms	CTGACAGATGCTCTCTTGGG	CACAACCCCAGAAACAGACA
CXCR4	Ms	GTCTATGTGGGCGTCTGGAT	GGCAGAGCTTTTGAACTTGG

(PBS/2%FBS). Dead cells were excluded from the analysis by 7-amino actinomycin D (7-AAD, eBioscience). Analysis was performed on an LSRFortessa flow cytometer by using FACS-Diva software (BD Bioscience). For detection of transgene expression by Ad vectors, EB-derived total cells or $CD41^{+}c\text{-}kit^{+}$ cells were transduced with Ad-DsRed or Ad-CA-GFP, respectively, for 1.5 h. At 48 h of incubation with the hematopoietic cytokines as described above, transgene expression in the cells was analyzed by flow cytometry.

Colony assay

A colony-forming assay was performed by plating ES cell-derived hematopoietic cells or iPS cell-derived hematopoietic cells into methylcellulose medium M3434 (Stem Cell Technologies, Vancouver, BC, Canada). After incubation at 37 °C and 5% CO_2 for 10 to 14 days in a humidified atmosphere, colony numbers were counted. The morphology of colonies was observed using an inverted light microscope.

RT-PCR

Total RNA was isolated with the use of ISOGENE (Nippon Gene, Tokyo, Japan). cDNA was synthesized by using Super-Script II reverse transcriptase (Invitrogen) and the oligo(dT) primer. Semi-quantitative PCR was performed with the use of TaKaRa ExTaq HS DNA polymerase (Takara, Shiga, Japan). The PCR conditions were 94 °C for 2 min, followed by the appropriate number of cycles of 94 °C for 15 s, 55 °C for 30 s with 72 °C for 30 s and a final extension of 72 °C for 1 min, except for the addition of 5% dimethyl sulfoxide in the case of hHoxB4 cDNA amplification. The product was assessed by 2% agarose gel electrophoresis followed by ethidium bromide staining. Quantitative real-time PCR was performed using StepOnePlus real-time PCR system with FAST SYBR Green Master Mix (Applied Biosystems, Foster-City, CA). The sequences of the primers used for in this study are listed in Table 1.

Supplementary materials related to this article can be found online at doi:10.1016/j.scr.2011.09.001.

Conflict of interest

The authors have no financial conflict of interest.

Acknowledgments

We thank Dr. S. Yamanaka for kindly providing the mouse iPS cell line 38C2 and 20D17. We would also like to thank Dr. J. Miyazaki and Dr. T. Imai for providing the CA promoter and anti-mouse CAR monoclonal antibody, respectively. We also thank Dr. K. Nishikawa (National Institute of Biomedical Innovation) for helpful comments. This work was supported by grants from the Ministry of Education, Culture, Sports, Science, and Technology (MEXT) of Japan and the Ministry of Health, Labour, and Welfare of Japan.

References

Arai, F., Hirao, A., Ohmura, M., Sato, H., Matsuoka, S., Takubo, K., Ito, K., Koh, G.Y., Suda, T., 2004. Tie2/angiopoietin-1 signaling regulates hematopoietic stem cell quiescence in the bone marrow niche. Cell 118, 149–161.

Bergelson, J.M., Cunningham, J.A., Droguett, G., Kurt-Jones, E.A., Krithivas, A., Hong, J.S., Horwitz, M.S., Crowell, R.L., Finberg, R.W., 1997. Isolation of a common receptor for Coxsackie B viruses and adenoviruses 2 and 5. Science 275, 1320–1323.

Bowles, K.M., Vallier, L., Smith, J.R., Alexander, M.R., Pedersen, R.A., 2006. HOXB4 overexpression promotes hematopoietic development by human embryonic stem cells. Stem Cells 24, 1359–1369.

Carson, S.D., 2000. Limited proteolysis of the coxsackievirus and adenovirus receptor (CAR) on HeLa cells exposed to trypsin. FEBS Lett. 484, 149–152.

Chadwick, K., Wang, L., Li, L., Menendez, P., Murdoch, B., Rouleau, A., Bhatia, M., 2003. Cytokines and BMP-4 promote hematopoietic differentiation of human embryonic stem cells. Blood 102, 906–915.

Evans, M.J., Kaufman, M.H., 1981. Establishment in culture of pluripotential cells from mouse embryos. Nature 292, 154–156.

Godin, I., Cumano, A., 2002. The hare and the tortoise: an embryonic haematopoietic race. Nat. Rev. Immunol. 2, 593–604.

Hacein-Bey-Abina, S., Von Kalle, C., Schmidt, M., McCormack, M.P., Wulffraat, N., Leboulch, P., Lim, A., Osborne, C.S., Pawliuk, R., Morillon, E., Sorensen, R., Forster, A., Fraser, P., Cohen, J.I., de Saint Basile, G., Alexander, I., Wintergerst, U., Frebourg, T., Aurias, A., Stoppa-Lyonnet, D., Romana, S., Radford-Weiss, I., Gross, F., Valensi, F., Delabesse, E., Macintyre, E., Sigaux, F., Soulier, J., Leiva, L.E., Wissler, M., Prinz, C., Rabbitts, T.H., Le Deist, F., Fischer, A., Cavazzana-Calvo, M., 2003. LMO2-associated clonal T cell proliferation in two patients after gene therapy for SCID-X1. Science 302, 415–419.

Inamura, M., Kawabata, K., Takayama, K., Tashiro, K., Sakurai, F., Katayama, K., Toyoda, M., Akutsu, H., Miyagawa, Y., Okita, H., Kiyokawa, N., Umezawa, A., Hayakawa, T., Furue, M.K., Mizuguchi, H., 2011. Efficient generation of hepatoblasts from human ES cells and iPS cells by transient overexpression of homeobox gene HEX. Mol. Ther. 19, 400–407.

Kawabata, K., Sakurai, F., Yamaguchi, T., Hayakawa, T., Mizuguchi, H., 2005. Efficient gene transfer into mouse embryonic stem cells with adenovirus vectors. Mol. Ther. 12, 547–554.

Keller, G., 2005. Embryonic stem cell differentiation: emergence of a new era in biology and medicine. Genes Dev. 19, 1129–1155.

Kim, K., Doi, A., Wen, B., Ng, K., Zhao, R., Cahan, P., Kim, J., Aryee, M.J., Ji, H., Ehrlich, L.I., Yabuuchi, A., Takeuchi, A., Cunniff, K.C., Hongguang, H., McKinney-Freeman, S., Naveiras, O., Yoon, T.J., Irizarry, R.A., Jung, N., Seita, J., Hanna, J., Murakami, P., Jaenisch, R., Weissleder, R., Orkin, S.H., Weissman, I.L., Feinberg, A.P., Daley, G.Q., 2010. Epigenetic memory in induced pluripotent stem cells. Nature 467, 285–290.

Kulkeaw, K., Horio, Y., Mizuochi, C., Ogawa, M., Sugiyama, D., 2010. Variation in hematopoietic potential of induced pluripotent stem cell lines. Stem Cell Rev. 6, 381–389.

Kurita, R., Sasaki, E., Yokoo, T., Hiroyama, T., Takasugi, K., Imoto, H., Izawa, K., Dong, Y., Hashiguchi, T., Soda, Y., Maeda, T., Suehiro, Y., Tanioka, Y., Nakazaki, Y., Tani, K., 2006. Tal1/Scl gene transduction using a lentiviral vector stimulates highly efficient hematopoietic cell differentiation from common marmoset (*Callithrix jacchus*) embryonic stem cells. Stem Cells 24, 2014–2022.

Kyba, M., Perlingeiro, R.C., Daley, G.Q., 2002. HoxB4 confers definitive lymphoid-myeloid engraftment potential on embryonic stem cell and yolk sac hematopoietic progenitors. Cell 109, 29–37.

Li, Z., Dullmann, J., Schiedlmeier, B., Schmidt, M., von Kalle, C., Meyer, J., Forster, M., Stocking, C., Wahlers, A., Frank, O., Ostertag, W., Kuhlcke, K., Eckert, H.G., Fehse, B., Baum, C., 2002. Murine leukemia induced by retroviral gene marking. Science 296, 497.

Maizel Jr., J.V., White, D.O. , Scharff, M.D., 1968. The polypeptides of adenovirus. I. Evidence for multiple protein components in the virion and a comparison of types 2, 7A, and 12. Virology 36, 115–125.

Matsumoto, K., Isagawa, T., Nishimura, T., Ogaeri, T., Eto, K., Miyazaki, S., Miyazaki, J., Aburatani, H., Nakauchi, H., Ema, H., 2009. Stepwise development of hematopoietic stem cells from embryonic stem cells. PLoS One 4, e4820.

McKinney-Freeman, S.L., Naveiras, O., Yates, F., Loewer, S., Philitas, M., Curran, M., Park, P.J., Daley, G.Q., 2009. Surface antigen phenotypes of hematopoietic stem cells from embryos and murine embryonic stem cells. Blood 114, 268–278.

Mikkola, H.K., Fujiwara, Y., Schlaeger, T.M., Traver, D., Orkin, S.H., 2003. Expression of CD41 marks the initiation of definitive hematopoiesis in the mouse embryo. Blood 101, 508–516.

Mitjavila-Garcia, M.T., Cailleret, M., Godin, I., Nogueira, M.M., Cohen-Solal, K., Schiavon, V., Lecluse, Y., Le Pesteur, F., Lagrue, A.H., Vainchenker, W., 2002. Expression of CD41 on hematopoietic progenitors derived from embryonic hematopoietic cells. Development 129, 2003–2013.

Mizuguchi, H., Kay, M.A., 1998. Efficient construction of a recombinant adenovirus vector by an improved in vitro ligation method. Hum. Gene Ther. 9, 2577–2583.

Mizuguchi, H., Kay, M.A., 1999. A simple method for constructing E1- and E1/E4-deleted recombinant adenoviral vectors. Hum. Gene Ther. 10, 2013–2017.

Nakano, T., Kodama, H., Honjo, T., 1994. Generation of lymphohematopoietic cells from embryonic stem cells in culture. Science 265, 1098–1101.

Niwa, H., Yamamura, K., Miyazaki, J., 1991. Efficient selection for high-expression transfectants with a novel eukaryotic vector. Gene 108, 193–199.

Okabe, M., Otsu, M., Ahn, D.H., Kobayashi, T., Morita, Y., Wakiyama, Y., Onodera, M., Eto, K., Ema, H., Nakauchi, H., 2009. Definitive proof for direct reprogramming of hematopoietic cells to pluripotency. Blood 114, 1764–1767.

Okita, K., Ichisaka, T., Yamanaka, S., 2007. Generation of germline-competent induced pluripotent stem cells. Nature 448, 313–317.

Pilat, S., Carotta, S., Schiedlmeier, B., Kamino, K., Mairhofer, A., Will, E., Modlich, U., Steinlein, P., Ostertag, W., Baum, C., Beug, H., Klump, H., 2005. HOXB4 enforces equivalent fates of ES-cell-derived and adult hematopoietic cells. Proc. Natl. Acad. Sci. U. S. A. 102, 12101–12106.

Polo, J.M., Liu, S., Figueroa, M.E., Kulalert, W., Eminli, S., Tan, K.Y., Apostolou, E., Stadtfeld, M., Li, Y., Shioda, T., Natesan, S., Wagers, A.J., Melnick, A., Evans, T., Hochedlinger, K., 2010. Cell type of origin influences the molecular and functional properties of mouse induced pluripotent stem cells. Nat. Biotechnol. 28, 848–855.

Schiedlmeier, B., Santos, A.C., Ribeiro, A., Moncaut, N., Lesinski, D., Auer, H., Kornacker, K., Ostertag, W., Baum, C., Mallo, M., Klump, H., 2007. HOXB4's road map to stem cell expansion. Proc. Natl. Acad. Sci. U. S. A. 104, 16952–16957.

Schmitt, T.M., de Pooter, R.F., Gronski, M.A., Cho, S.K., Ohashi, P.S., Zuniga-Pflucker, J.C., 2004. Induction of T cell development and establishment of T cell competence from embryonic stem cells differentiated in vitro. Nat. Immunol. 5, 410–417.

Takahashi, K., Yamanaka, S., 2006. Induction of pluripotent stem cells from mouse embryonic and adult fibroblast cultures by defined factors. Cell 126, 663–676.

Takahashi, K., Tanabe, K., Ohnuki, M., Narita, M., Ichisaka, T., Tomoda, K., Yamanaka, S., 2007. Induction of pluripotent stem cells from adult human fibroblasts by defined factors. Cell 131, 861–872.

Tashiro, K., Kawabata, K., Sakurai, H., Kurachi, S., Sakurai, F., Yamanishi, K., Mizuguchi, H., 2008. Efficient adenovirus vector-mediated PPAR gamma gene transfer into mouse embryoid bodies promotes adipocyte differentiation. J. Gene Med. 10, 498–507.

Tashiro, K., Inamura, M., Kawabata, K., Sakurai, F., Yamanishi, K., Hayakawa, T., Mizuguchi, H., 2009. Efficient adipocyte and osteoblast differentiation from mouse induced pluripotent stem cells by adenoviral transduction. Stem Cells 27, 1802–1811.

Tashiro, K., Kawabata, K., Inamura, M., Takayama, K., Furukawa, N., Sakurai, F., Katayama, K., Hayakawa, T., Furue, M.K., Mizuguchi, H., 2010. Adenovirus vector-mediated efficient transduction into human embryonic and induced pluripotent stem cells. Cell. Reprogram. 12, 501–507.

Thomson, J.A., Itskovitz-Eldor, J., Shapiro, S.S., Waknitz, M.A., Swiergiel, J.J., Marshall, V.S., Jones, J.M., 1998. Embryonic stem cell lines derived from human blastocysts. Science 282, 1145–1147.

Tomko, R.P., Xu, R., Philipson, L., 1997. HCAR and MCAR: the human and mouse cellular receptors for subgroup C adenoviruses and group B coxsackieviruses. Proc. Natl. Acad. Sci. U. S. A. 94, 3352–3356.

Vodyanik, M.A., Bork, J.A., Thomson, J.A., Slukvin, I.I., 2005. Human embryonic stem cell-derived CD34+ cells: efficient production in the coculture with OP9 stromal cells and analysis of lymphohematopoietic potential. Blood 105, 617–626.

Wang, Y., Yates, F., Naveiras, O., Ernst, P., Daley, G.Q., 2005. Embryonic stem cell-derived hematopoietic stem cells. Proc. Natl. Acad. Sci. U. S. A. 102, 19081–19086.

Williams, D., Baum, C., 2004. Gene therapy needs both trials and new strategies. Nature 429, 129.

Zhang, X.B., Beard, B.C., Trobridge, G.D., Wood, B.L., Sale, G.E., Sud, R., Humphries, R.K., Kiem, H.P., 2008. High incidence of leukemia in large animals after stem cell gene therapy with a HOXB4-expressing retroviral vector. J. Clin. Invest. 118, 1502–1510.

Biomaterials 34 (2013) 1781–1789

Contents lists available at SciVerse ScienceDirect

Biomaterials

journal homepage: www.elsevier.com/locate/biomaterials

3D spheroid culture of hESC/hiPSC-derived hepatocyte-like cells for drug toxicity testing

Kazuo Takayama [a,b], Kenji Kawabata [b,c], Yasuhito Nagamoto [a,b], Keisuke Kishimoto [a,b], Katsuhisa Tashiro [b], Fuminori Sakurai [a], Masashi Tachibana [a], Katsuhiro Kanda [d], Takao Hayakawa [e], Miho Kusuda Furue [f,g], Hiroyuki Mizuguchi [a,b,h,*]

[a] Laboratory of Biochemistry and Molecular Biology, Graduate School of Pharmaceutical Sciences, Osaka University, Osaka 565-0871, Japan
[b] Laboratory of Stem Cell Regulation, National Institute of Biomedical Innovation, Osaka 567-0085, Japan
[c] Laboratory of Biomedical Innovation, Graduate School of Pharmaceutical Sciences, Osaka University, Osaka 565-0871, Japan
[d] Pharma Business Project, Corporate Projects Center, Corporate Strategy Division, Hitachi High-Technologies Corporation, Ibaraki 312-8504, Japan
[e] Pharmaceutical Research and Technology Institute, Kinki University, Osaka 577-8502, Japan
[f] Laboratory of Embryonic Stem Cell Cultures, Department of Disease Bioresources Research, National Institute of Biomedical Innovation, Osaka 567-0085, Japan
[g] Department of Embryonic Stem Cell Research, Field of Stem Cell Reseach, Institute for Frontier Medical Sciences, Kyoto University, Kyoto 606-8507, Japan
[h] The Center for Advanced Medical Engineering and Informatics, Osaka University, Osaka 565-0871, Japan

ARTICLE INFO

Article history:
Received 11 September 2012
Accepted 20 November 2012
Available online 8 December 2012

Keywords:
Hepatocyte-like cell
Human ES cell
Human iPS cell
Nanopillar plate
Drug screening

ABSTRACT

Although it is expected that hepatocyte-like cells differentiated from human embryonic stem (ES) cells or induced pluripotent stem (iPS) cells will be utilized in drug toxicity testing, the actual applicability of hepatocyte-like cells in this context has not been well examined so far. To generate mature hepatocyte-like cells that would be applicable for drug toxicity testing, we established a hepatocyte differentiation method that employs not only stage-specific transient overexpression of hepatocyte-related transcription factors but also a three-dimensional spheroid culture system using a Nanopillar Plate. We succeeded in establishing protocol that could generate more matured hepatocyte-like cells than our previous protocol. In addition, our hepatocyte-like cells could sensitively predict drug-induced hepatotoxicity, including reactive metabolite-mediated toxicity. In conclusion, our hepatocyte-like cells differentiated from human ES cells or iPS cells have potential to be applied in drug toxicity testing.

© 2012 Elsevier Ltd. All rights reserved.

1. Introduction

Hepatocyte-like cells that are generated from human embryonic stem cells (hESCs) [1] or human induced pluripotent stem cells (hiPSCs) [2] are expected to be used in drug screening instead of primary (or cryopreserved) human hepatocytes (PHs). We recently demonstrated that stage-specific transient transduction of transcription factors, in addition to treatment with optimal growth factors and cytokines, is useful for promoting hepatic differentiation [3–6]. The hepatocyte-like cells, which have many hepatocyte characteristics (the abilities to uptake low-density lipoprotein and Indocyanine green, store glycogen, and synthesize urea) and drug metabolism capacity, were generated from hESCs/hiPSCs by combinational transduction of FOXA2 and HNF1α [6]. However, further maturation of the hepatocyte-like cells is required because their hepatic characteristics, such as drug metabolism capacity, are lower than those of PHs [6].

To promote further maturation of the hepatocyte-like cells, we subjected them to three-dimensional (3D) spheroid cultures. It is known that various 3D culture conditions (such as Algimatrix scaffolds [7], cell sheet technology [8], galactose-carrying substrata [9], and basement membrane substratum [10]) are useful for the maturation of the hepatocyte-like cells. Nanopillar Plate technology [11] used in the present study makes it easy to control the configuration of the spheroids. The Nanopillar Plate has an arrayed μm-scale hole structure at the bottom of each well, and nanopillars were aligned further at the bottom of the respective holes. The seeded cells evenly drop into the holes, then migrate and aggregate on top surface of the nanopillars, thus likely to form the uniform spheroids in each hole. Not only 3D spheroid cultures [12] but also Matrigel overlay cultures [13] are useful for maintaining the hepatocyte characteristics of PHs. Therefore, we employed both 3D

* Corresponding author. Laboratory of Biochemistry and Molecular Biology, Graduate School of Pharmaceutical Sciences, Osaka University, 1-6 Yamadaoka, Suita, Osaka 565-0871, Japan. Tel.: +81 6 6879 8185; fax: +81 6 6879 8186.
E-mail address: mizuguch@phs.osaka-u.ac.jp (H. Mizuguchi).

0142-9612/$ – see front matter © 2012 Elsevier Ltd. All rights reserved.
http://dx.doi.org/10.1016/j.biomaterials.2012.11.029

spheroid culture and Matrigel overlay culture systems to promote hepatocyte maturation of the hepatocyte-like cells.

The hepatocyte-like cells generated from hESCs/hiPSCs are expected to be used in drug development. To the best of our knowledge, however, few studies have tried to predict widespread drug-induced cytotoxicity *in vitro* using the hepatocyte-like cells. To precisely determine the applicability of the hepatocyte-like cells to drug screening, it is necessary to investigate the responses of these hepatocyte-like cells to many kinds of hepatotoxic drugs.

In this study, 3D spheroid and Matrigel overlay cultures of the hepatocyte-like cells were performed to promote hepatocyte maturation. The gene expression analysis of cytochrome P450 (CYP) enzymes, conjugating enzymes, hepatic transporters, and hepatic nuclear receptors in the 3D spheroid-cultured hESC- or hiPSC-derived hepatocyte-like cells (3D ES-hepa or 3D iPS-hepa), were analyzed. In addition, CYP induction potency and drug metabolism capacity were estimated in the 3D ES/iPS-hepa. To determine the suitability of these cells for drug screening, we examined whether the drug-induced cytotoxicity is induced by treatment of various kinds of hepatotoxic drugs in 3D ES/iPS-hepa.

2. Materials and methods

2.1. hESCs and hiPSCs culture

A hESC line, H1 and H9 (WiCell Research Institute), was maintained on a feeder layer of mitomycin C-treated mouse embryonic fibroblasts (Millipore) with Repro Stem medium (Repro CELL) supplemented with 5 ng/ml fibroblast growth factor 2 (FGF2) (Sigma). Both H1 and H9 were used following the Guidelines for Derivation and Utilization of Human Embryonic Stem Cells of the Ministry of Education, Culture, Sports, Science and Technology of Japan and furthermore, and the study was approved by Independent Ethics Committee.

Three human iPSC lines were provided from the JCRB Cell Bank (Tic, JCRB Number: JCRB1331; Dotcom, JCRB Number: JCRB1327; Toe, JCRB Number: JCRB1338) [14,15]. These human iPSC lines were maintained on a feeder layer of mitomycin C-treated mouse embryonic fibroblasts with iPSellon (Cardio) supplemented with 10 ng/ml FGF2. Other three human iPSC lines, 201B6, 201B7 and 253G1 were kindly provided by Dr. S. Yamanaka (Kyoto University) [2]. These human iPSC lines were maintained on a feeder layer of mitomycin C-treated mouse embryonic fibroblasts with Repro Stem supplemented with 5 ng/ml FGF2.

2.2. In vitro differentiation

Before the initiation of cellular differentiation, the medium of hESCs was exchanged into a defined serum-free medium, hESF9, and cultured as previously reported [16]. The differentiation protocol for the induction of definitive endoderm cells, hepatoblasts, and hepatocytes was based on our previous reports with some modifications [3–5,17]. Briefly, in mesendoderm differentiation, hESCs were dissociated into single cells by using Accutase (Millipore) and cultured for 2 days on Matrigel (BD Biosciences) in differentiation hESF-DIF medium which contains 100 ng/ml Activin A (R&D Systems) and 10 ng/ml bFGF (hESF-DIF medium was purchased from Cell Science & Technology Institute; differentiation hESF-DIF medium was supplemented with 10 μg/ml human recombinant insulin, 5 μg/ml human apotransferrin, 10 μM 2-mercaptoethanol, 10 μM ethanolamine, 10 μM sodium selenite, and 0.5 mg/ml bovine fatty acid free serum albumin [all from sigma]). To generate definitive endoderm cells, the mesendoderm cells were transduced with 3000 vector particle (VP)/cell of Ad-FOXA2 for 1.5 h on day 2 and cultured until day 6 on Matrigel in differentiation hESF-DIF medium supplemented with 100 ng/ml Activin A and 10 ng/ml bFGF. For induction of hepatoblasts, the DE cells were transduced with each 1500 VP/cell of Ad-FOXA2 and Ad-HNF1α for 1.5 h on day 6 and cultured for 3 days on Matrigel in hepatocyte culture medium (HCM) (Lonza) supplemented with 30 ng/ml bone morphogenetic protein 4 (BMP4) (R&D Systems) and 20 ng/ml FGF4 (R&D Systems). In hepatic expansion, the hepatoblasts were transduced with each 1500 VP/cell of Ad-FOXA2 and Ad-HNF1α for 1.5 h on day 9 and cultured for 3 days on Matrigel in HCM supplemented with 10 ng/ml hepatocyte growth factor (HGF), 10 ng/ml FGF1, 10 ng/ml FGF4, and 10 ng/ml FGF10 (all from R&D Systems). To perform hepatocyte maturation on Nanopillar Plate (a prototype multi-well culturing plate for spheroid culture developed and prepared by Hitachi High-Technologies Corporation) shown in Fig. 1B, the cells were seeded at 2.5×10^5 cells/cm^2 (Fig. S1) in hepatocyte culture medium (Fig. S2) supplemented with 10 ng/ml HGF, 10 ng/ml FGF1, 10 ng/ml FGF4, and 10 ng/ml FGF10 on day 11. In the first stage of hepatocyte maturation (from day 12 to day 25), the cells were cultured for 13 days on Matrigel in HCM supplemented with 20 ng/ml HGF, 20 ng/ml oncostatin M (OsM), 10 ng/ml FGF4, and 10^{-6} M dexamethasone (DEX). In the second stage of hepatocyte maturation (from day 25 to day 35), Matrigel was overlaid on the hepatocyte-like cells. Matrigel were diluted to a final concentration of 0.25 mg/ml with William's E medium (Invitrogen) containing 4 mM L-glutamine, 50 ug/ml gentamycin sulfate, 1 × ITS (BD Biosciences), 20 ng/ml OsM, and 10^{-6} M DEX. The culture medium was aspirated, and then the Matrigel solution (described above) was overlaid on the hepatocyte-like cells. The cells were incubated overnight, and the medium was replaced with HCM supplemented with 20 ng/ml OsM and 10^{-6} M DEX.

2.3. Adenovirus (Ad) vectors

Ad vectors were constructed by an improved *in vitro* ligation method [18,19]. The human EF-1α promoter-driven LacZ-, FOXA2-, or HNF1α-expressing Ad vectors (Ad-LacZ, Ad-FOXA2, or Ad-HNF1α, respectively) were constructed previously [3,4,20]. All of Ad vectors contain a stretch of lysine residue (K7) peptides in the C-terminal region of the fiber knob for more efficient transduction of hESCs, hiPSCs, and DE cells, in which transfection efficiency was almost 100%, and purified as described previously [3–5]. The vector particle (VP) titer was determined by using a spectrophotometric method [21].

2.4. Flow cytometry

Single-cell suspensions of hESC/hiPSC-derived cells were fixed with 2% paraformaldehyde (PFA) at 4°C for 20 min, and then incubated with the primary antibody (described in Table S1), followed by the secondary antibody (described in Table S1). Flow cytometry analysis was performed using a FACS LSR Fortessa flow cytometer (BD Biosciences).

2.5. RNA isolation and reverse transcription-polymerase chain reaction (RT-PCR)

Total RNA was isolated from hESCs or hiPSCs and their derivatives using ISOGENE (Nippon Gene). cDNA was synthesized using 500 ng of total RNA with a Superscript VILO cDNA synthesis kit (Invitrogen). Real-time RT-PCR was performed with Taqman gene expression assays (Applied Biosystems) or SYBR Premix Ex Taq (TaKaRa) using an ABI PRISM 7000 Sequence Detector (Applied Biosystems). Relative quantification was performed against a standard curve and the values were normalized against the input determined for the housekeeping gene, glyceraldehyde 3-phosphate dehydrogenase (GAPDH). The primer sequences used in this study are described in Table S2.

2.6. Immunohistochemistry

The cells were fixed with 4% PFA. After incubation with 1% Triton X-100, blocking with Blocking One (Nakalai tesque), the cells were incubated with primary antibody (describe in Table S1) at 4°C for over night, followed by incubation with a secondary antibody (described in Table S1) at room temperature for 1 h.

2.7. ELISA

The hESCs or hiPSCs were differentiated into hepatocytes as described in Fig. 1A. The culture supernatants, which were incubated for 24 h after fresh medium was added, were collected and analyzed for the amount of ALB secretion by ELISA. ELISA kits for ALB were purchased from Bethyl. ELISA was performed according to the manufacturer's instructions. The amount of ALB secretion was calculated according to each standard followed by normalization to the protein content per well.

2.8. Urea secretion

The hESCs or hiPSCs were differentiated into hepatocytes as described in Fig. 1A. The culture supernatants, which were incubated for 24 h after fresh medium was added, were collected and analyzed for the amount of urea secretion. Urea measurement kits were purchased from BioAssay Systems. The experiment was performed according to the manufacturer's instructions. The amount of urea secretion was calculated according to each standard followed by normalization to the protein content per well.

2.9. Canalicular secretory assay

At cellular differentiation, the hepatocyte-like cell spheroids were treated with 5 mM choly-lysyl-fluorescein (CLF) (BD Biosciences) for 30 min. The cells were washed with culture medium, and then observed by fluorescence microscope. To inhibit the function of BSEP, the cells were pretreated with Cyclosporin A 24 h before of the CLF treatment.

2.10. Assay for CYP activity and CYP induction

To measure the cytochrome P450 2C9 and 3A4 activity of the cells, we performed lytic assays by using a P450-GloTM CYP2C9 (catalog number; V8791) and

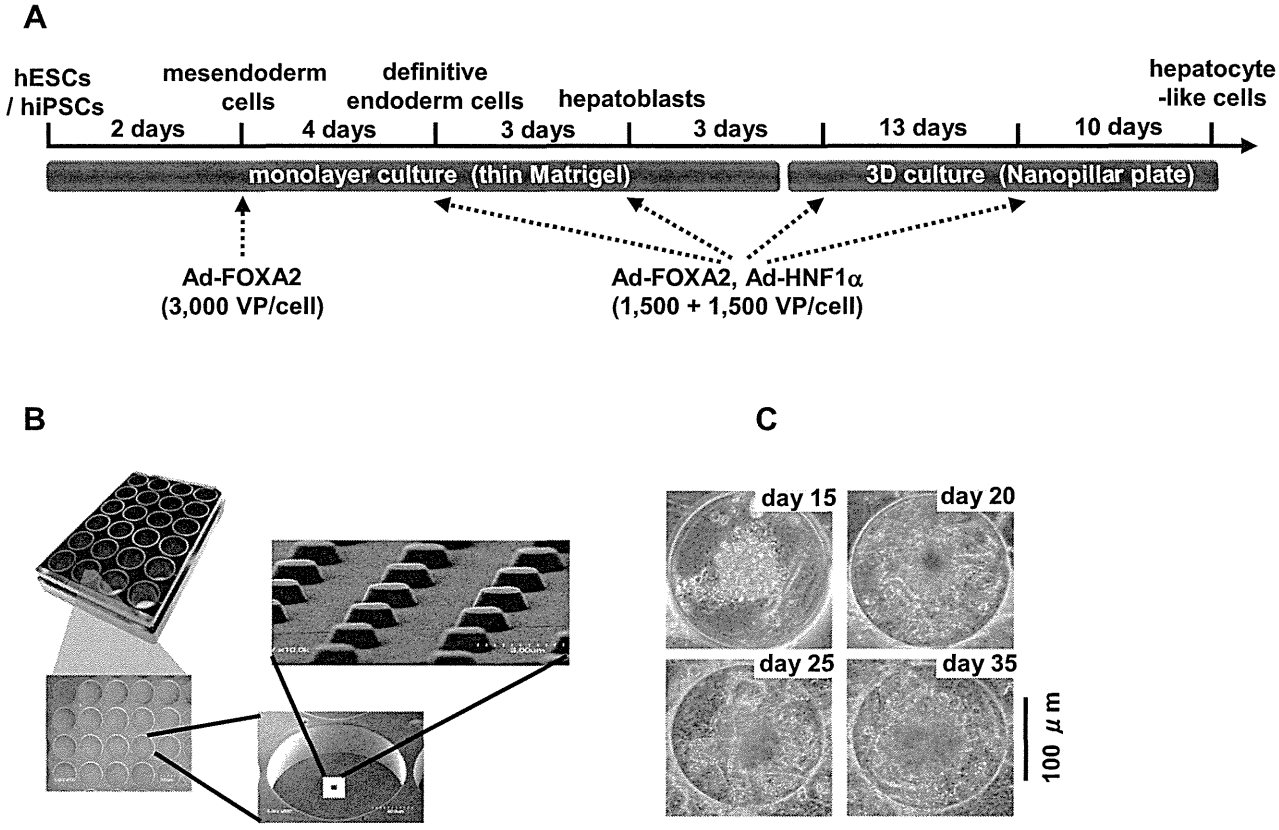

Fig. 1. Hepatocyte-like cells were differentiated from hESCs/hiPSCs by using Nanopillar Plate. (A) The procedure for differentiation of hESCs into 3D ES/iPS-hepa via mesendoderm cells, definitive endoderm cells, and hepatoblasts is presented schematically. In the differentiation, not only the addition of growth factors but also stage-specific transient transduction of both FOXA2- and HNF1α-expressing Ad vector (Ad-FOXA2 and Ad-HNF1α, respectively) was performed. The cellular differentiation procedure is described in detail in the materials and methods section. (B) Photograph display of a 24-well format Nanopillar Plate and its microstructural appearances of the hole and pillar structure. (C) Phase-contrast micrographs of the hESC-hepa spheroids on the Nanopillar Plate are shown. Scale bar represents 100 μm.

3A4 (catalog number; V9001) Assay Kit (Promega), respectively. We measured the fluorescence activity with a luminometer (Lumat LB 9507; Berthold) according to the manufacturer's instructions. The CYP activity was normalized with the protein content per well.

To measure CYP2C9 and 3A4 induction potency, the CYP activity was measured by using a P450-GloTM CYP2C9 and 3A4 Assay Kit, respectively. The cells were treated with rifampicin, which is known to induce both CYP2C9 and 3A4, at a final concentration of 10 μM for 48 h. The cells were also treated with Ketoconazole (Sigma) or Sulfaphenazole (Sigma), which are inhibitors for CYP3A4 or 2C9, at a final concentration of 1 μM or 2 μM, respectively, for 48 h. Controls were treated with DMSO (final concentration 0.1%). Inducer compounds were replaced daily.

2.11. Cell viability tests

Cell viability was assessed by the WST-8 assay kit (Dojindo) in Fig. 2D. After treatment with test compounds, such as Acetaminophen (Wako), Allopurinol (Wako), Amiodaron (Sigma), Benzbromarone (Sigma), Clozapine (Wako), Cyclizine (MP bio), Dantrolene (Wako), Desipramine (Wako), Disufliram (Wako), Erythromycin (Wako), Felbamate (Sigma), Flutamide (Wako), Isoniazid (Sigma), Labetalol (Sigma), Lefunomide (Sigma), Maprotiline (Sigma), Nefazodone (Sigma), Nitrofurantoin (Sigma), Sulindac (Wako), Tacrine (Sigma), Tebinafine (Wako), Tolcapone (TRC), Troglitazone (Wako), and Zafirlukast (Cayman) for 24 h, the cell viability was measured. The cell viability of the 3D iPSC-hepa were assessed by WST-8 assay after 24 h exposure to different concentrations of Aflatoxin B1 (Sigma) and Benzbromarone in the presence or absence of the CYP3A4 or 2C9 inhibitor, Ketoconazole (1 μM) or Sulfaphenazole (10 μM), respectively. The control refers to incubations in the absence of test compounds and was considered as 100% viability value. Controls were treated with DMSO (final concentration 0.1%). ATP assay (BioAssay Systems), Alamar Blue assay (Invitrogen), and Crystal Violet (Wako) staining assay were performed according to the manufacturer's instructions.

2.12. Primary human hepatocytes

Three lots of cryopreserved human hepatocytes (lot Hu8072 [CellzDirect], HC2-14, and HC10-101 [Xenotech]) were used. These three lots of crypreserved human hepatocytes were cultured according to our previous report [5].

2.13. Statistical analysis

Statistical analysis was performed using the unpaired two-tailed Student's *t*-test. All data are represented as means ± SD ($n = 3$).

3. Results

The 3D ES/iPS-hepa were generated from hESCs/hiPSCs as shown in Fig. 1A. Hepatocyte differentiation of hESCs/hiPSCs was efficiently promoted by stage-specific transient transduction of FOXA2 and HNF1α in addition to the treatment with appropriate soluble factors (growth factors and cytokines) [6]. On day 11, the hESC-derived cells were seeded at 2.5×10^5 cells/cm^2 (Fig. S1) on Nanopillar Plate (Fig. 1B), in hepatocyte culture medium (Fig. S2) to promote hepatocyte maturation. In addition, Matrigel was overlaid on the 3D ES-hepa to promote further hepatocyte maturation. The 3D ES-hepa with compact morphology that were adhesive to the substratum and had an optimal size (approximately 100 μm in diameter) were formed by using the Nanopillar Plate (Fig. 1C). The spheroids seem to be stable because they could be cultured for more than 20 days. We have confirmed that more than 90% of the cells that constitute the spheroids were alive, indicating that the necrotic centers are absent.

To investigate whether or not a 3D spheroid culture could promote hepatocyte maturation of the hepatocyte-like cells, various hepatocyte characteristics of the 3D ES/iPS-hepa were compared with those of the monolayer-cultured hESC- or hiPSC-derived hepatocyte-like cells (mono ES-hepa or mono iPS-hepa). The gene expression level of *ALB* peaked on day 20 in the mono ES-hepa, and then it was dramatically decreased after day 25 (Fig. 2A). In contrast, the gene expression level of *ALB* was

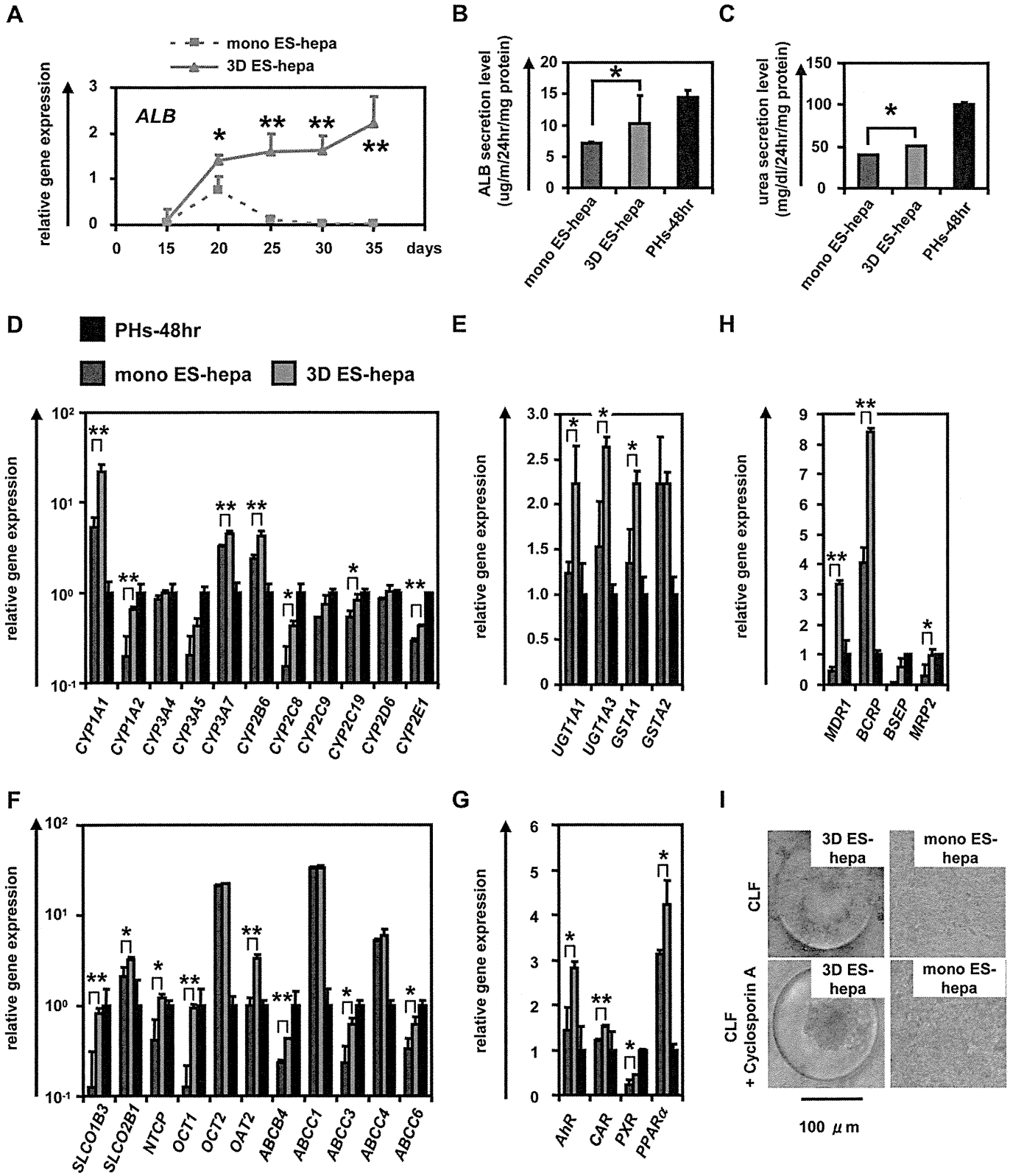

Fig. 2. Hepatocyte functions in hESC-derived hepatocyte-like cells were enhanced by using Nanopillar Plate. (A) The gene expression levels of *ALB* were measured by real-time RT-PCR on day 15, 20, 25, 30, and 35. On the *y* axis, the gene expression levels in PHs (three lots of PHs were used in all studies), which were cultured for 48 h after plating (PHs-48hr), were taken as 1.0. (B, C) The amount of ALB (B) and urea (C) secretion were examined in the mono ES-hepa (day 20), the 3D ES-hepa (day 35), and PHs-48hr. (D–H) The gene expression levels of CYP enzymes (D), conjugating enzymes (E), hepatic transporters (F), hepatic nuclear receptors (G), and bile canaliculi transporters (H) were examined by real-time RT-PCR in the mono ES-hepa, the 3D ES-hepa, and PHs-48hr. On the *y* axis, the expression levels in PHs-48hr were taken as 1.0. (I) The ability of bile acid uptake and efflux was examined in the mono ES-hepa and 3D ES-hepa. Choly-lysyl-fluorescein (CLF) (5 μM) was used for the observation of bile canaliculi uptake and efflux. To inhibit transportation by BSEP, the cells were pretreated with 1 μM Cyclosporin A. $^{*}P < 0.05$; $^{**}P < 0.01$.

moderately increased in the 3D ES-hepa until day 35 (Fig. 2A). These results suggest that the hepatocyte functions of the 3D ES-hepa are sustained for more than 2 weeks on the Nanopillar Plate, although those of the mono ES-hepa are rapidly devitalized (Fig. 2A and Fig. S4). Other hepatocyte characteristics, such as ability of ALB and urea secretion and gene expression levels of hepatocyte-related markers in the 3D ES-hepa were compared with those of the mono ES-hepa (Fig. 2B–H). Because the gene expression level of *ALB* in the 3D ES-hepa was the highest on day 35 and that in mono ES-hepa was the highest on day 20, various hepatocyte characteristics were compared on day 35 or day 20, respectively. The amount of ALB (Fig. 2B) and urea (Fig. 2C) secretion in the 3D ES-hepa was higher than those of the mono ES-hepa. The gene expression levels of CYP enzymes (Fig. 2D), conjugating enzymes (Fig. 2E), hepatic transporters (Fig. 2F), hepatic nuclear receptors (Fig. 2G), and hepatic transcription factors (Fig. S5) in the 3D ES-hepa were higher than those in the mono ES-hepa. The expression levels of most of the genes in the 3D ES-hepa were higher than those in the mono ES-hepa. Because the previous study [11] showed that hepatocyte spheroids expressed hepatocyte transporters similar to those of the bile canaliculi in native liver tissue, the gene expression levels of bile canaliculi transporters (Fig. 2H), as well as the ability of bile acid uptake and efflux, (Fig. 2I) were examined in the 3D ES-hepa. The gene expression levels of bile canaliculi transporters were increased in the 3D ES-hepa compared with those of mono ES-hepa and PHs (Fig. 2H). The bile canaliculi formation was visualized by BSEP fluorescent substrate: Cholyl-lysyl-fluorescein (CLF), which is inhibited by BSEP

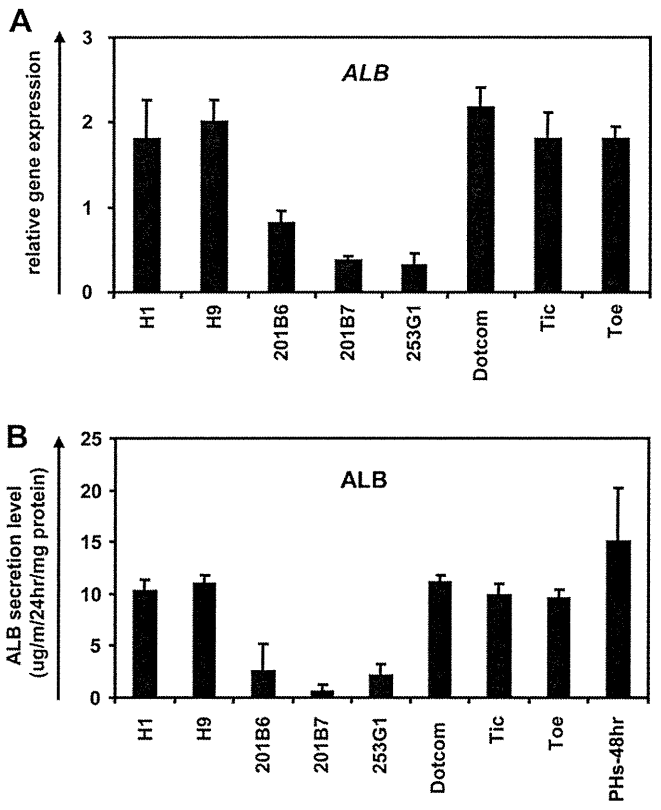

Fig. 3. Comparison of the hepatic differentiation capacities of various hESC and hiPSC lines hESCs (H1 and H9) and hiPSCs (201B6, 201B7, 253G1, Dotcom, Tic, and Toe) were differentiated into the 3D ES/iPS-hepa as described in Fig. 1A. (A) On day 20, the gene expression level of *ALB* was examined by real-time RT-PCR. On the *y* axis, the gene expression level of *ALB* in PHs-48hr was taken as 1.0. (B) On day 20, the amount of ALB secretion was examined by ELISA. The amount of ALB secretion was calculated according to each standard followed by normalization to the protein content per well.

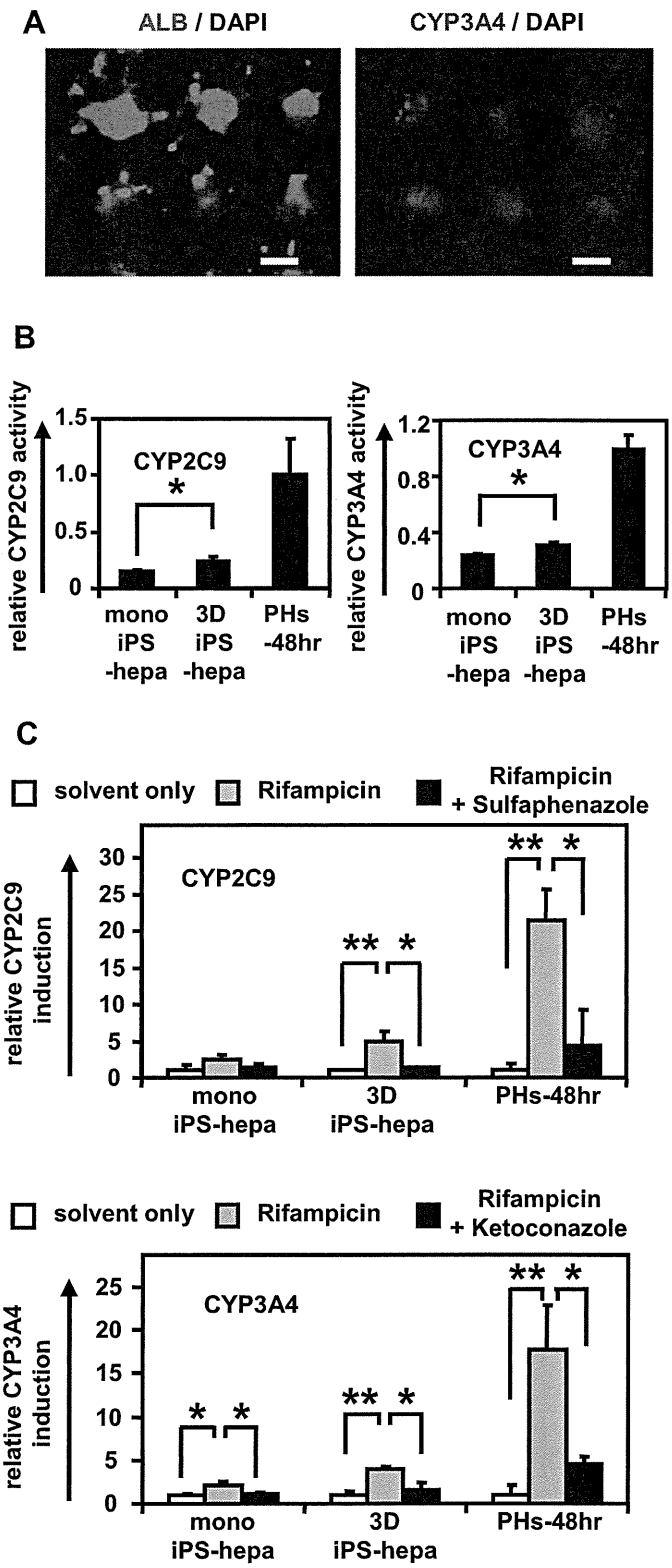

Fig. 4. Drug metabolism capacity and CYP induction potency were examined in the 3D iPS-hepa. (A) The 3D iPS-hepa (day 35) were subjected to immunostaining with anti-ALB (green) or CYP3A4 (red) antibodies. Nuclei were counterstained with DAPI (blue). Scale bar represents 100 μm. (B) The CYP activity was measured in the mono iPS-hepa (day 20), the 3D iPS-hepa (day 35), and PHs-48hr. On the *y* axis, the CYP activity in PHs-48hr was taken as 1.0. (C) Induction of CYP2C9 (left) or CYP3A4 (right) by DMSO (solvent only; white bar), Rifampicin (gray bar), or rifampicin and CYP inhibitor (Sulfaphenazole or Ketoconazole, black bar) in the mono iPS-hepa, the 3D iPS-hepa, and PHs-48hr. On the *y* axis, the CYP activity of the cells that have been cultured in DMSO-containing medium was taken as 1.0. $^{*}P < 0.05$; $^{**}P < 0.01$.

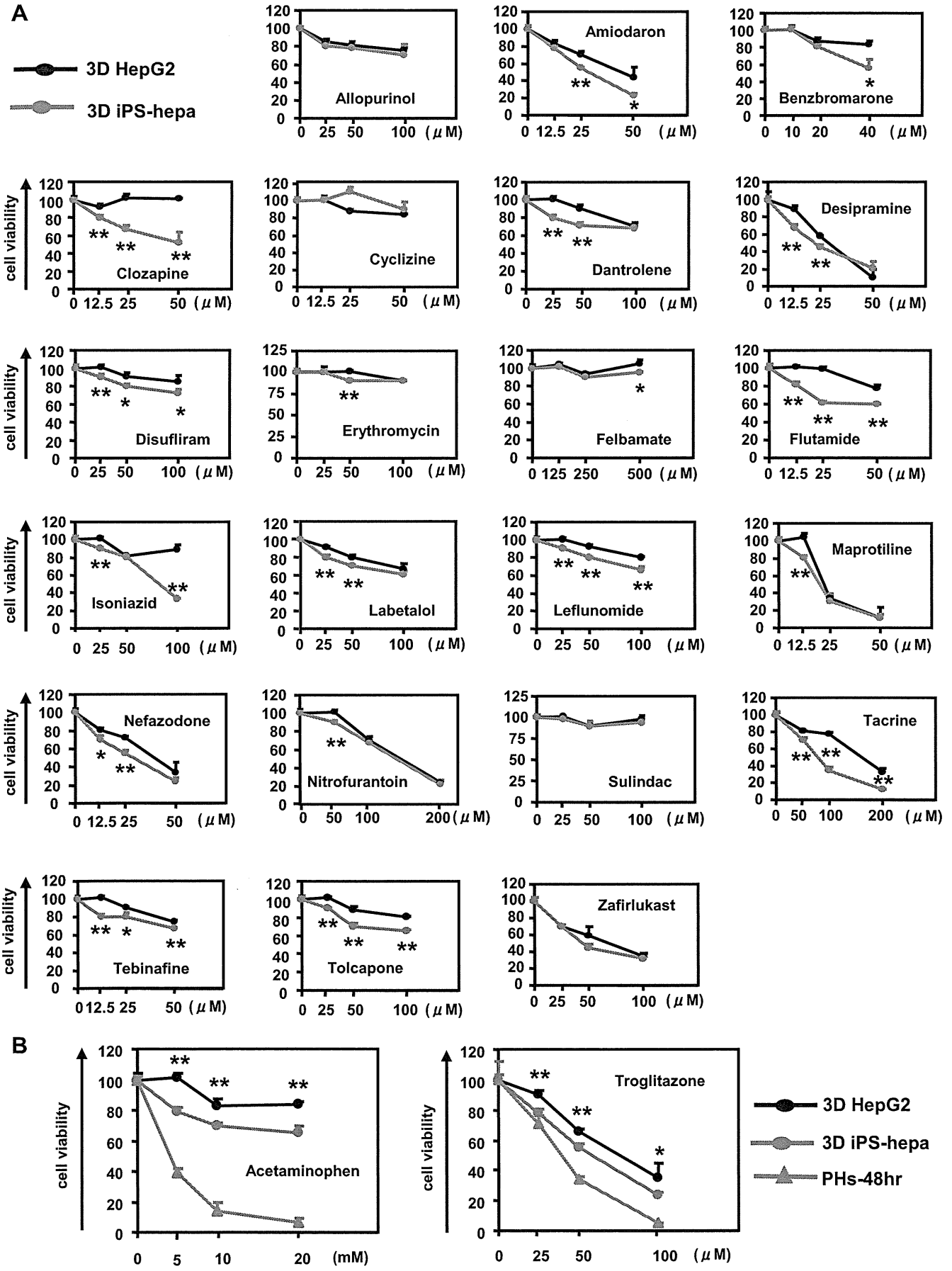
A
3D HepG2
3D iPS-hepa
cell viability
Allopurinol
Amiodaron
Benzbromarone
Clozapine
Cyclizine
Dantrolene
Desipramine
Disufliram
Erythromycin
Felbamate
Flutamide
Isoniazid
Labetalol
Leflunomide
Maprotiline
Nefazodone
Nitrofurantoin
Sulindac
Tacrine
Tebinafine
Tolcapone
Zafirlukast
B
Acetaminophen
Troglitazone
PHs-48hr
(μM)
(mM)

inhibitor Cyclosporin A [22,23]. More CLF was accumulated in the 3D ES-hepa than in the mono ES-hepa (Fig. 2I *upper panel*). Moreover, CLF accumulation was inhibited by Cyclosporin A treatment only in the 3D ES-hepa (Fig. 2I *lower panel*), demonstrating that the functionality of BSEP transporter in 3D ES-hepa was greater than that in mono ES-hepa. These results suggested that hepatocyte maturation was promoted by the culture on the Nanopillar Plate. It is likely that, compared to the monolayer culture condition, the 3D spheroid-culture condition is more similar to the *in vivo* condition.

It is important to select an hESC/hiPSC line that has a strong ability to differentiate into hepatocyte-like cells in the case of medical applications such as drug screening. In this study, two hESC lines and six hiPSC lines were differentiated into the hepatocyte-like cells, and then their gene expression levels of *ALB* (Fig. 3A) and ALB secretion levels (Fig. 3B) were compared. These results suggest that the iPSC line, Dotcom, was the suitable cell line for hepatocyte maturation. Therefore, the iPSC line, Dotcom, was used to examine the possibility of the 3D iPS-hepa for drug screening. The drug metabolism capacity and the CYP induction potency of the 3D iPS-hepa were compared with those of the mono iPS-hepa. We confirmed the expression of ALB and CYP3A4 protein in the 3D ES-hepa (Fig. 4A). The activity levels of CYP enzymes in the 3D iPS-hepa were measured according to the metabolism of the CYP2C9 or CYP3A4 substrates (Fig. 4B); the levels were higher than those of the mono iPS-hepa (Fig. 4B). We further tested the induction of CYP2C9 and CYP3A4 by chemical stimulation (rifampicin was used as a CYP2C9 or CYP3A4 inducer). Compared with mono iPS-hepa, the 3D iPS-hepa produced more metabolites in response to chemical stimulation (Fig. 4C). In addition, the CYP induction was inhibited by using CYP2C9 or CYP3A4 inhibitor (Sulfaphenazole or Ketoconazole, respectively). These results indicated that drug metabolism capacity and CYP induction potency in 3D iPS-hepa were higher than those in mono iPS-hepa.

Many researchers have tried to predict the drug-induced cytotoxicity *in vitro* using hepatocarcinoma-derived cells such as HepG2 cells [24,25]. HepG2 cells are less expensive than PHs and the reproducible experiments are easier to perform than they are with PHs, although 30% of the compounds were incorrectly classified as nontoxic [24,25]. To overcome these problems, hESC/hiPSC-derived hepatocyte-like cells are expected to be used to predict drug-induced cytotoxicity. To examine its applicability to drug screening, the 3D iPS-hepa were treated with various drugs, that cause hepatotoxicity. WST-8 assay was performed to evaluate cell viability (Fig. S6). The susceptibility of the 3D iPS-hepa to most of the hepatotoxic drugs was higher than that of the mono iPS-hepa (Fig. S7). Compared to the mono iPS-hepa, the 3D iPS-hepa were more suitable tools for drug screening. Next, the susceptibility of the 3D iPS-hepa to the hepatotoxic drugs was compared with that of the 3D spheroid cultured HepG2 cells (3D HepG2; the hepatocyte functions of 3D HepG2 cells are higher than those of monolayer cultured HepG2 cells [Fig. S8]). With most of the drugs, the cell viability of the 3D iPS-hepa was lower than that of the 3D HepG2 (Fig. 5A). These results indicated that the 3D iPS-hepa are more valuable tools for drug screening than the 3D HepG2. However, the susceptibility of the 3D iPS-hepa to Acetaminophen and Troglitazone was lower than that of the PHs which were cultured for 48 h after the cells were plated (Fig. 5B). These results might be due to the lower activity levels of CYPs in 3D iPS-hepa as compared as those in PHs. Taken together, 3D iPS-hepa are more valuable tools for drug screening than the 3D HepG2, although further maturation of 3D iPS-hepa is still required for 3D iPS-hepa to be an alternative cell source of PHs in the drug screening.

To examine whether drug-induced cytotoxicity is caused by CYP metabolites in 3D iPS-hepa, Aflatoxin B1 (mainly metabolized by CYP3A4 [26]) and Benzbromarone (mainly metabolized by CYP2C9 [27]) were treated in the presence or absence of a CYP3A4 and a 2C9 inhibitor, Ketoconazole and Sulfaphenazole, respectively (Fig. 6). The cell viability of 3D iPS-hepa was partially rescued by treatment with the CYP inhibitor. These results indicated that drug-induced cytotoxicity was caused by CYP metabolites of Aflatoxin B1 and Benzbromarone.

4. Discussion

Recently, it has been expected that human pluripotent stem cells and their derivatives, including hepatocyte-like cells, will be utilized in applications for the safety assessment of drugs. We have previously reported that combinational overexpression of SOX17, HEX, and HNF4α, or combinational overexpression of FOXA2 and HNF1α could promote hepatocyte differentiation [5,6]. However, the drug metabolism capacity of the hepatocyte-like cells generated by our previous protocol was still lower than that of primary human hepatocytes [6]. To generate more matured hepatocyte-like cells as compared with our previous protocol, we established a hepatocyte differentiation method employing not only stage-specific transient overexpression of hepatocyte-related transcription factors but also a 3D culture systems using a Nanopillar Plate, was established. Although the use of hepatocyte-like cells generated from hESCs/hiPSCs in application for drug toxicity testing has begun to be focused, to the best of our knowledge, there have been few studies that have investigated whether hepatocyte-like cells could predict many kinds of drug-induced toxicity.

3D culture spheroids were generated from hESCs/hiPSCs by using a Nanopillar Plate. The diameter of the spheroids was approximately 100 μm on day 35 of differentiation (Fig. 1C). Because it is known that the no-oxygen limitation would take place in spheroids up to 100 μm in diameter [28], the size of the spheroid might be important to generate spheroids with high viability. A Nanopillar Plate has a potential to regulate the spheroid diameter simply by culturing under optimized seeding condition, on its suitably designed pillar and hole structure [11]. Therefore, a Nanopillar Plate would be a suitable environment for the generation of 3D ES/iPS-hepa that show high viability and possess high level of hepatocellular functions.

The levels of many hepatocyte functions, such as ALB secretion ability (Fig. 2B), urea secretion ability (Fig. 2C), hepatocyte-related gene expressions (Fig. 2D–H), drug metabolism capacity (Fig. 4B), and CYP induction potency (Fig. 4C), of 3D ES/iPS-hepa were higher than those of mono ES/iPS-hepa. This might have been because the structural and functional polarity, which can be seen in the naïve environment of hepatocytes, of the hepatocyte-like cells was configured by a 3D culturing condition. Previous studies have shown that a 3D culture condition is suitable to maintain the hepatic characteristics of the isolated hepatocytes because this condition mimic *in vivo* environment [29,30]. These facts indicated that the 3D culture condition is a more suitable condition for the hepatocyte-like cells than the monolayer culture condition.

Two hES cell lines and six hiPS cell lines were differentiated into the hepatocyte-like cells in this study. The hiPS cell line, Dotcom, seemed to be a suitable cell line for hepatic differentiation (Fig. 3). Because the hepatic differentiation propensity differs among the

Fig. 5. The possibility of applying 3D iPS-hepa to drug testing was examined. (A) The cell viability of the 3D HepG2 (black) and 3D iPSC-hepa (red) were assessed by WST-8 assay after 24 h exposure to different concentrations of 22 test compounds. (B) The cell viability of the 3D HepG2 (black), 3D iPSC-hepa (red), and PHs-48hr (green) were assessed by WST-8 assay after 24 h exposure to different concentrations of Acetaminophen and Troglitazone. Cell viability is expressed as a percentage of cells treated with solvent only. $^{*}P < 0.05$; $^{**}P < 0.01$.

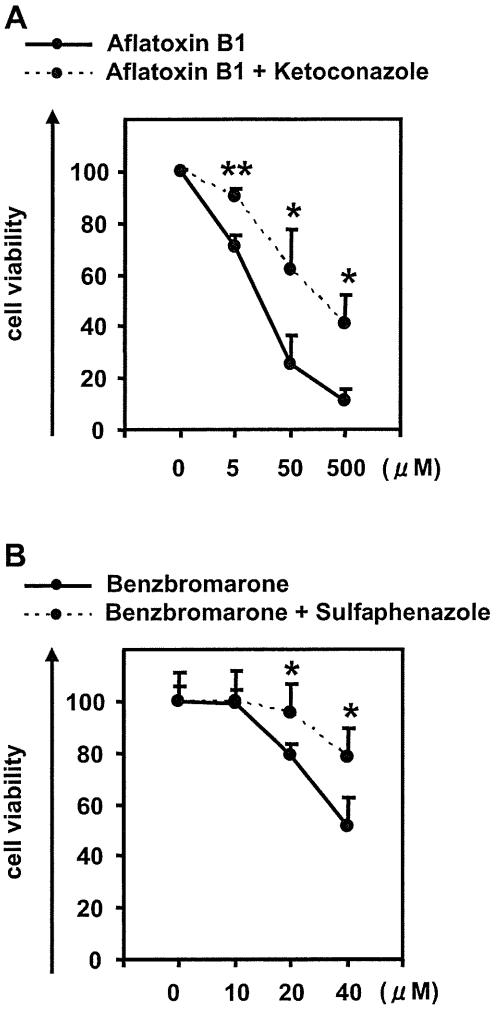

Fig. 6. Drug-induced cytotoxicity in the 3D iPS-hepa is mediated by cytochrome P450. (A, B) The cell viability of the 3D iPSC-hepa was assessed by WST-8 assay after 24 h exposure to different concentrations of (A) Aflatoxin B1 and (B) Benzbromarone in the presence or absence of the CYP3A4 or 2C9 inhibitor, Ketoconazole or Sulfaphenazole, respectively. Cell viability was expressed as the percentage of cells treated with solvent only. $^{*}P < 0.05$; $^{**}P < 0.01$.

hES/hiPS cell lines, it would be important to select an appropriate cell line for medical applications such as drug screening. However, the dominant reason for this hepatic differentiation propensity is not been well known. It would be interesting study to elucidate the mechanism of this propensity.

Although the drug metabolism capacity and CYP induction potency of 3D iPS-hepa were higher than those of mono iPS-hepa (Fig. 4B and C), they were still lower than those of primary human hepatocytes. The hepatic nuclear factors are known to be key molecules in the CYP induction of hepatocytes [30]. Therefore, overexpression of hepatic nuclear factors, which are not abundantly expressed in the hepatocyte-like cells (such as *PXR*), might upregulate the CYP induction potency of the hepatocyte-like cells.

3D iPS-hepa were more sensitive for detection of the drug-induced cytotoxicity than HepG2 cells that are widely used to predict hepatotoxicity [31,32] (Fig. 5). In addition, the decrease of cell viability, which was caused by hepatotoxic drugs, of 3D iPS-hepa was partially rescued by treatment with a CYP inhibitor (Fig. 6). These data suggest that the hepatocyte-like cells could detect the toxicity of the reactive metabolites that were generated by drug metabolizing enzymes such as CYP enzymes. Because in many cases, drug-induced hepatotoxicity is caused by the reactive metabolites produced by drug metabolizing enzymes [33], our finding that the hepatocyte-like cells could detect the toxicity of reactive metabolites should be of great potential for toxicological screening. Moreover, it might be possible to predict idiosyncratic liver toxicity by using hepatocyte-like cells generated from hiPSCs that were established from a patient with a rare CYP polymorphism. However, some compounds did not show any cytotoxicity (such as Cyclizine, Felbamate, and Sulindac) (Fig. 5). To apply the hepatocyte-like cells for wide-spread drug screening, generation of the hepatocyte-like cells are required to detect hepatotoxity in more sensitive manner. Previous studies showed that the depletion of conjugating enzymes [32] or knockdown of Nrf2 [34] expression are useful to upregulate the sensitivity to hepatotoxic drugs. Therefore, these approaches would be useful to generate more sensitive hepatocytes to toxic drugs.

5. Conclusions

In this study, we established the efficient hepatocyte differentiation method which employs not only stage-specific transient overexpression of hepatocyte-related transcription factors but also 3D spheroid culture systems by using Nanopillar Plate. To the best of our knowledge, this is the first study in which the hepatocyte-like cells, having enough hepatocyte functions, mediate drug-induced cytotoxicity against many compounds. Our hepatocyte-like cells differentiated from hESCs or hiPSCs have potential to be applied in drug toxicity testing.

Acknowledgments

We thank Misae Nishijima and Hiroko Matsumura for their excellent technical support. HM, KK, MKF, and TH were supported by grants from the Ministry of Health, Labor, and Welfare of Japan. HM was also supported by Japan Research foundation For Clinical Pharmacology, and The Uehara Memorial Foundation. MKF was also supported by Japan Society for the Promotion of Science Grant-in-Aid for Scientific Research. FS was supported by Program for Promotion of Fundamental Studies in Health Sciences of the National Institute of Biomedical Innovation (NIBIO). We thank Hiromu Yamada (NIBIO) for helpful discussion.

Appendix A. Supplementary data

Supplementary data related to this article can be found at http://dx.doi.org/10.1016/j.biomaterials.2012.11.029.

References

[1] Thomson JA, Itskovitz-Eldor J, Shapiro SS, Waknitz MA, Swiergiel JJ, Marshall VS, et al. Embryonic stem cell lines derived from human blastocysts. Science 1998;282:1145–7.
[2] Takahashi K, Tanabe K, Ohnuki M, Narita M, Ichisaka T, Tomoda K, et al. Induction of pluripotent stem cells from adult human fibroblasts by defined factors. Cell 2007;131:861–72.
[3] Inamura M, Kawabata K, Takayama K, Tashiro K, Sakurai F, Katayama K, et al. Efficient generation of hepatoblasts from human ES cells and iPS cells by transient overexpression of homeobox gene HEX. Mol Ther 2011;19:400–7.
[4] Takayama K, Inamura M, Kawabata K, Tashiro K, Katayama K, Sakurai F, et al. Efficient and directive generation of two distinct endoderm lineages from human ESCs and iPSCs by differentiation stage-specific SOX17 transduction. PLoS One 2011;6:e21780.
[5] Takayama K, Inamura M, Kawabata K, Katayama K, Higuchi M, Tashiro K, et al. Efficient generation of functional hepatocytes from human embryonic stem cells and induced pluripotent stem cells by HNF4alpha transduction. Mol Ther 2012;20:127–37.
[6] Takayama K, Inamura M, Kawabata K, Sugawara M, Kikuchi K, Higuchi M, et al. Generation of metabolically functioning hepatocytes from human pluripotent stem cells by FOXA2 and HNF1alpha transduction. J Hepatol 2012;57:628–36.
[7] Ramasamy TS, Yu JS, Selden C, Hodgson H, Cui W. Application of three-dimensional culture conditions to human embryonic stem cell-derived

definitive endoderm cells enhances hepatocyte differentiation and functionality. Tissue Eng Part A. http://dx.doi.org/10.1089/ten.tea.2012.0190. Available from URL: http://www.ncbi.nlm.nih.gov/pubmed/23003670; 2012.
[8] Nagamoto Y, Tashiro K, Takayama K, Ohashi K, Kawabata K, Sakurai F, et al. The promotion of hepatic maturation of human pluripotent stem cells in 3D co-culture using type I collagen and Swiss 3T3 cell sheets. Biomaterials 2012;33:4526–34.
[9] Meng Q, Haque A, Hexig B, Akaike T. The differentiation and isolation of mouse embryonic stem cells toward hepatocytes using galactose-carrying substrata. Biomaterials 2012;33:1414–27.
[10] Shiraki N, Yamazoe T, Qin Z, Ohgomori K, Mochitate K, Kume K, et al. Efficient differentiation of embryonic stem cells into hepatic cells in vitro using a feeder-free basement membrane substratum. PLoS One 2011;6:e24228.
[11] Takahashi R, Sonoda H, Tabata Y, Hisada A. Formation of hepatocyte spheroids with structural polarity and functional bile canaliculi using nanopillar sheets. Tissue Eng Part A 2010;16:1983–95.
[12] Tong JZ, Sarrazin S, Cassio D, Gauthier F, Alvarez F. Application of spheroid culture to human hepatocytes and maintenance of their differentiation. Biol Cell 1994;81:77–81.
[13] Bi YA, Kazolias D, Duignan DB. Use of cryopreserved human hepatocytes in sandwich culture to measure hepatobiliary transport. Drug Metab Dispos 2006;34:1658–65.
[14] Makino H, Toyoda M, Matsumoto K, Saito H, Nishino K, Fukawatase Y, et al. Mesenchymal to embryonic incomplete transition of human cells by chimeric OCT4/3 (POU5F1) with physiological co-activator EWS. Exp Cell Res 2009;315:2727–40.
[15] Nagata S, Toyoda M, Yamaguchi S, Hirano K, Makino H, Nishino K, et al. Efficient reprogramming of human and mouse primary extra-embryonic cells to pluripotent stem cells. Genes Cells 2009;14:1395–404.
[16] Furue MK, Na J, Jackson JP, Okamoto T, Jones M, Baker D, et al. Heparin promotes the growth of human embryonic stem cells in a defined serum-free medium. Proc Natl Acad Sci U S A 2008;105:13409–14.
[17] Kawabata K, Inamura M, Mizuguchi H. Efficient hepatic differentiation from human iPS cells by gene transfer. Methods Mol Biol 2012;826:115–24.
[18] Mizuguchi H, Kay MA. Efficient construction of a recombinant adenovirus vector by an improved in vitro ligation method. Hum Gene Ther 1998;9:2577–83.
[19] Mizuguchi H, Kay MA. A simple method for constructing E1- and E1/E4-deleted recombinant adenoviral vectors. Hum Gene Ther 1999;10:2013–7.
[20] Tashiro K, Kawabata K, Sakurai H, Kurachi S, Sakurai F, Yamanishi K, et al. Efficient adenovirus vector-mediated PPAR gamma gene transfer into mouse embryoid bodies promotes adipocyte differentiation. J Gene Med 2008;10:498–507.
[21] Maizel Jr JV, White DO, Scharff MD. The polypeptides of adenovirus. I. Evidence for multiple protein components in the virion and a comparison of types 2, 7A, and 12. Virology 1968;36:115–25.
[22] Yasumiba S, Tazuma S, Ochi H, Chayama K, Kajiyama G. Cyclosporin A reduces canalicular membrane fluidity and regulates transporter function in rats. Biochem J 2001;354:591–6.
[23] Roman ID, Fernandez-Moreno MD, Fueyo JA, Roma MG, Coleman R. Cyclosporin A induced internalization of the bile salt export pump in isolated rat hepatocyte couplets. Toxicol Sci 2003;71:276–81.
[24] Rodriguez-Antona C, Donato MT, Boobis A, Edwards RJ, Watts PS, Castell JV, et al. Cytochrome P450 expression in human hepatocytes and hepatoma cell lines: molecular mechanisms that determine lower expression in cultured cells. Xenobiotica 2002;32:505–20.
[25] Hewitt NJ, Hewitt P. Phase I and II enzyme characterization of two sources of HepG2 cell lines. Xenobiotica 2004;34:243–56.
[26] Gallagher EP, Kunze KL, Stapleton PL, Eaton DL. The kinetics of aflatoxin B1 oxidation by human cDNA-expressed and human liver microsomal cytochromes P450 1A2 and 3A4. Toxicol Appl Pharmacol 1996;141:595–606.
[27] Lee MH, Graham GG, Williams KM, Day RO. A benefit-risk assessment of benzbromarone in the treatment of gout. Was its withdrawal from the market in the best interest of patients? Drug Saf 2008;31:643–65.
[28] Glicklis R, Merchuk JC, Cohen S. Modeling mass transfer in hepatocyte spheroids via cell viability, spheroid size, and hepatocellular functions. Biotechnol Bioeng 2004;86:672–80.
[29] Kim K, Ohashi K, Utoh R, Kano K, Okano T. Preserved liver-specific functions of hepatocytes in 3D co-culture with endothelial cell sheets. Biomaterials 2012;33:1406–13.
[30] Khetani SR, Bhatia SN. Microscale culture of human liver cells for drug development. Nat Biotechnol 2008;26:120–6.
[31] Iwamura A, Fukami T, Hosomi H, Nakajima M, Yokoi T. CYP2C9-mediated metabolic activation of losartan detected by a highly sensitive cell-based screening assay. Drug Metab Dispos 2011;39:838–46.
[32] Hosomi H, Akai S, Minami K, Yoshikawa Y, Fukami T, Nakajima M, et al. An in vitro drug-induced hepatotoxicity screening system using CYP3A4-expressing and gamma-glutamylcysteine synthetase knockdown cells. Toxicol In Vitro 2010;24:1032–8.
[33] Guengerich FP, MacDonald JS. Applying mechanisms of chemical toxicity to predict drug safety. Chem Res Toxicol 2007;20:344–69.
[34] Hosomi H, Fukami T, Iwamura A, Nakajima M, Yokoi T. Development of a highly sensitive cytotoxicity assay system for CYP3A4-mediated metabolic activation. Drug Metab Dispos 2011;39:1388–95.

Research Article

EASL EUROPEAN ASSOCIATION FOR THE STUDY OF THE LIVER | JOURNAL OF HEPATOLOGY

Generation of metabolically functioning hepatocytes from human pluripotent stem cells by FOXA2 and HNF1α transduction

Kazuo Takayama[1,2], Mitsuru Inamura[1,2], Kenji Kawabata[2,3], Michiko Sugawara[4], Kiyomi Kikuchi[4], Maiko Higuchi[2], Yasuhito Nagamoto[1,2], Hitoshi Watanabe[1,2], Katsuhisa Tashiro[2], Fuminori Sakurai[1], Takao Hayakawa[5,6], Miho Kusuda Furue[7,8], Hiroyuki Mizuguchi[1,2,9,*]

[1]*Laboratory of Biochemistry and Molecular Biology, Graduate School of Pharmaceutical Sciences, Osaka University, Osaka 565-0871, Japan;* [2]*Laboratory of Stem Cell Regulation, National Institute of Biomedical Innovation, Osaka 567-0085, Japan;* [3]*Laboratory of Biomedical Innovation, Graduate School of Pharmaceutical Sciences, Osaka University, Osaka 565-0871, Japan;* [4]*Tsukuba Laboratories, Eisai Co., Ltd., Ibaraki 300-2635, Japan;* [5]*Pharmaceutics and Medical Devices Agency, Tokyo 100-0013, Japan;* [6]*Pharmaceutical Research and Technology Institute, Kinki University, Osaka 577-8502, Japan;* [7]*Laboratory of Cell Cultures, Department of Disease Bioresources Research, National Institute of Biomedical Innovation, Osaka 567-0085, Japan;* [8]*Laboratory of Cell Processing, Institute for Frontier Medical Sciences, Kyoto University, Kyoto 606-8507, Japan;* [9]*The Center for Advanced Medical Engineering and Informatics, Osaka University, Osaka 565-0871, Japan*

Background & Aims: Hepatocyte-like cells differentiated from human embryonic stem cells (hESCs) and induced pluripotent stem cells (hiPSCs) can be utilized as a tool for screening for hepatotoxicity in the early phase of pharmaceutical development. We have recently reported that hepatic differentiation is promoted by sequential transduction of SOX17, HEX, and HNF4α into hESC- or hiPSC-derived cells, but further maturation of hepatocyte-like cells is required for widespread use of drug screening.

Methods: To screen for hepatic differentiation-promoting factors, we tested the seven candidate genes related to liver development.

Results: The combination of two transcription factors, FOXA2 and HNF1α, promoted efficient hepatic differentiation from hESCs and hiPSCs. The expression profile of hepatocyte-related genes (such as genes encoding cytochrome P450 enzymes, conjugating enzymes, hepatic transporters, and hepatic nuclear receptors) achieved with FOXA2 and HNF1α transduction was comparable to that obtained in primary human hepatocytes. The hepatocyte-like cells generated by FOXA2 and HNF1α transduction exerted various hepatocyte functions including albumin and urea secretion, and the uptake of indocyanine green and low density lipoprotein. Moreover, these cells had the capacity to metabolize all nine tested drugs and were successfully employed to evaluate drug-induced cytotoxicity.

Conclusions: Our method employing the transduction of FOXA2 and HNF1α represents a useful tool for the efficient generation of metabolically functional hepatocytes from hESCs and hiPSCs, and the screening of drug-induced cytotoxicity.

Keywords: FOXA2; HNF1α; Hepatocytes; Adenovirus; Drug screening; Drug metabolism; hESCs; hiPSCs.

Received 14 November 2011; received in revised form 31 March 2012; accepted 4 April 2012; available online 29 May 2012

* Corresponding author. Address: Laboratory of Biochemistry and Molecular Biology, Graduate School of Pharmaceutical Sciences, Osaka University, 1-6 Yamadaoka, Suita, Osaka 565-0871, Japan. Tel.: +81 6 6879 8185; fax: +81 6 6879 8186.

E-mail address: mizuguch@phs.osaka-u.ac.jp (H. Mizuguchi).

© 2012 European Association for the Study of the Liver. Published by Elsevier B.V. All rights reserved.

Introduction

Hepatocyte-like cells differentiated from human embryonic stem cells (hESCs) [1] or human induced pluripotent stem cells (hiPSCs) [2] have more advantages than primary human hepatocytes (PHs) for drug screening. While application of PHs in drug screening has been hindered by lack of cellular growth, loss of function, and de-differentiation *in vitro* [3], hESC- or hiPSC-derived hepatocyte-like cells (hESC-hepa or hiPSC-hepa, respectively) have potential to solve these problems.

Hepatic differentiation from hESCs and hiPSCs can be divided into four stages: definitive endoderm (DE) differentiation, hepatic commitment, hepatic expansion, and hepatic maturation. Various growth factors are required to mimic liver development [4] and to promote hepatic differentiation. Previously, we showed that transduction of transcription factors in addition to treatment with optimal growth factors was effective to enhance hepatic differentiation [5–7]. An almost homogeneous hepatocyte population was obtained by sequential transduction of SOX17, HEX, and HNF4α into hESC- or hiPSCs-derived cells [7]. However, further maturation of the hESC-hepa and hiPSC-hepa is required for widespread use of drug screening because the drug metabolism capacity of these cells was not sufficient.

In some previous reports, hESC-hepa and hiPSC-hepa have been characterized for their hepatocyte functions in numerous ways, including functional assessment such as glycogen storage and low density lipoprotein (LDL) uptake [7]. To make a more precise judgment as to whether hESC-hepa and hiPSC-hepa can be applied to drug screening, it is more important to assess cytochrome P450 (CYP) induction potency and drug metabolism capacity rather than general hepatocyte function. Although Duan *et al.* have examined the drug metabolism capacity of hESC-hepa, drug metabolites were measured at 24 or 48 h [8]. To precisely